10% fetal calf serum (FCS). The human hepatoma cell line Huh7, harboring the full genome of the HCV Con1 strain (genotype 1b), was prepared as described by Pietschmann et al.[31] We also established an Huh7 cell line harboring the subgenome of the JFH1 strain by the transfection of the plasmid pSGR-JFH1.[32] The Huh7-derived cell lines harboring a full length HCV replicon were maintained in DMEM containing 10% FCS, nonessential amino acids, sodium pyruvate, and 1 mg/mL G418 (Nakarai Tesque, Tokyo, Japan). The viral RNA of JFH1 was introduced into Huh7OK1 as described by Wakita et al.[33] The viral RNA of JFH1 derived from the plasmid pJFH1 was prepared as described by Wakita et al.[33]

### Statistical Analysis

Experiments for RNAi transfection and qRT-PCR were performed three times. The estimated values were represented as the mean ± standard deviation ($n$ = 3). The significance of differences in the means was determined by the Student's $t$ test.

## RESULTS AND DISCUSSION

### Core Expression and PA28γ Knockout Induce Substantial Changes in the Expression Levels of Host Proteins Associated with HCV Infection in the Liver

The PowerBlot immunoblots showed proteins with increased or decreased levels (defined as those that displayed >1.8-fold change in abundance) in the transgenic samples relative to the WT samples and also relative to each other. In all, we identified 37 proteins with increased levels and 15 proteins with decreased levels in CoreTGvsWT, 24 proteins with increased levels and 15 proteins with decreased levels in PA28$\gamma^{-/-}$-CoreTGvsWT, and 26 proteins with increased levels and 36 proteins with decreased levels in PA28$\gamma^{-/-}$CoreTGvsCoreTG. While most proteins with altered abundance display changes between 1.8-fold and 6-fold, some proteins displayed much higher fold changes. For instance, WRN protein levels increased 17-fold in CoreTGvsWT (Table 1).

Our analysis detected changes in the abundance of proteins, known to be associated with HCV pathogenesis, in the liver samples from CoreTG compared with WT. These include Arginase I (ARG1; +2.08-fold), a liver enzyme associated with the polyamine metabolism, which is known to be overexpressed in HCV-mediated hepatocarcinogenesis;[34] STAT3 (+2.30-fold), which is directly activated by the Core and HCV-mediated oxidative stress facilitating tumorigenesis and is also essential for HCV replication;[35−37] STAT1 (+2-fold), which interacts with Core and facilitates the HCV-mediated attenuation of the host interferon signaling;[38] and MAPK14 (p38 MAPK; −2.81-fold), which is cooperatively activated by Core and ethanol in HCV infection[39] (Table 1). These results are in line with the previous observations that Core expression can induce HCV pathogenesis and hepatocarcinogenesis in transgenic mice.[2] Among other examples, BIN1, which interacts with the HCV NS5A protein and contributes to the pathogenesis of HCC,[40] was suppressed 1.88-fold in PA28$\gamma^{-/-}$CoreTGvsCoreTG; this is consistent with the lack of HCC pathogenesis in PA28$\gamma^{-/-}$CoreTG mice. Similar studies have aimed to characterize the global changes in the host transcriptome and proteome in response to HCV infection.[41−44] These studies, however, have not provided specific insights into PA28γ's roles in HCV pathogenesis. Our observations suggest that the PowerBlot assay was able to capture successfully some of the molecular signatures associated with the Core-PA28γ interplay in HCV pathogenesis.

### Topological Analysis of the Extended Protein Interaction Networks

To further understand the biological significance of the differential protein levels, we retrieved PPIs for the proteins with increased and decreased levels in CoreTGvsWT, PA28$\gamma^{-/-}$CoreTGvsWT, and PA28$\gamma^{-/-}$CoreTGvsCoreTG and inferred the corresponding extended protein interaction networks for each data set using TargetMine (see Materials and Methods). First, we computed the *node degree distribution* and *characteristic/average path length* measures to capture the topology of the extended PPI networks as described earlier.[22] The degree of a protein, which corresponds to the number of its interacting partners, may often reflect its biological relevance since a better connected protein may have a higher ability of influencing biological networks via PPIs. Average path lengths provide an approximate measure of the relative ease and speed of transfer of information between the proteins in a network. The CoreTGvsWT extended network was made up of 1373 entities (proteins) with 12535 interactions, the PA28$\gamma^{-/-}$CoreTGvsWT extended network of 1057 entities with 8988 interactions, and the PA28$\gamma^{-/-}$CoreTGvsCoreTG of 1476 entities with 12871 interactions between them, respectively (Tables S3, S4). For comparison, we also derived an extended PPI network for all the non-genetic PPIs in the human genome as compiled in BioGRID and iRefindex repositories (data not shown). The average degree (defined as the number of interactions for a given protein) of the CoreTGvsWT (17.31), PA28$\gamma^{-/-}$CoreTGvsWT (16.1), and PA28$\gamma^{-/-}$CoreTGvsCoreTG (16.57) extended networks was higher than the degree inferred for the human interactome (10.17). This observation suggests that HCV infection targets several highly connected cellular proteins with an ability to influence a large number of host factors in HCV pathogenesis. The average (shortest) path lengths of the three extended networks (2.93, 2.9, and 2.97, respectively) were significantly shorter than that inferred for the human interactome (3.88), suggesting that the Core and PA28γ influenced cellular networks are more compact and inclined toward faster communication between the constituents relative to the human interactome (Figure 1). Our observations are consistent with previous studies on the protein interaction networks associated with HCV infection.[22,45]

The compactness of the HCV-influenced protein networks coupled with the ability to influence a wide array of factors in the host cellular networks may facilitate a rapid propagation of the signaling information and allow the virus to respond rapidly to the host mobilization against HCV infection.

### Functional Analysis of the Extended Protein Interaction Networks

Next, we investigated the extended networks for the enrichment of specific biological associations (KEGG pathways, GO terms, and OMIM phenotypes, Tables S5, S6, and S7). The analysis of the CoreTGvsWT, PA28$\gamma^{-/-}$CoreTGvsWT, and PA28$\gamma^{-/-}$CoreTGvsCoreTG extended networks revealed an enrichment ($p \leq 0.05$) of 116, 104, and 118 KEGG pathways, respectively (Table S5). Below we describe our observations on the selected enriched biological themes of interest, chiefly associated with the PA28$\gamma^{-/-}$CoreTGvsCoreTG network. Functional associations for the host factors previously known to be associated with HCV pathogenesis and HCC are

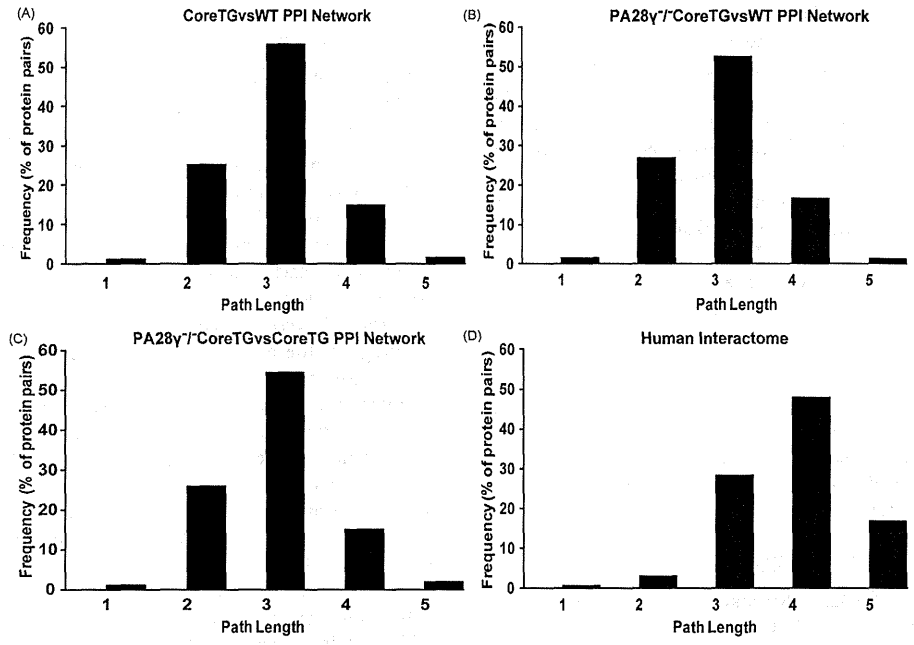


**Figure 1.** Graphical representation of the shortest path length distribution for (A) CoreTGvsWT extended network, (B) PA28$\gamma^{-/-}$CoreTGvsWT extended network, (C) PA28$\gamma^{-/-}$CoreTGvsCoreTG extended network, and (D) human protein interactome. The path length is represented on the *x*-axis, while the *y*-axis describes the frequency, i.e., the percentage of node (protein) pairs within the PPI network with a given shortest path length. For simplicity, only the node frequencies for path lengths 1–5 are displayed.

summarized in Table 2. Specific functional associations for the CoreTGvsWT and PA28$\gamma^{-/-}$CoreTGvsWT networks, except when discussed below, are detailed in the Supporting Information. It will highlight the biological significance of the differentially expressed proteins, their interactions, and their probable roles in HCV infection and help identify potentially novel regulators of and biomarkers for HCV pathogenesis.

### Vesicular Transport

HCV infection involves the formation of the HCV replication complex in the detergent-resistant membrane (DRM) fraction or lipid rafts. These subcellular membrane fractions are utilized by some pathogens including viruses to facilitate viral entry and assembly.[46−49] HCV infection induces modifications in the host lipid raft proteome, which directly impacts HCV replication in the infected cells.[50] Core targeting to the early and late endosomes and the viral particle production requires the components of the endosome-based secretory pathways.[51,52]

**CoreTGvsWT Extended Network.** The PowerBlot analysis revealed the two endosomal proteins VTI1A and STX8 (KEGG Pathway "SNARE interactions in vesicular transport"; $p = 0.023$; Table S5) that were upregulated 3.25- and 1.88-fold, respectively, in CoreTGvsWT (Table 1). SNAREs are membrane-anchored proteins involved in membrane trafficking.[53] Some SNAREs may function in HCV egress by possibly facilitating the fusion of the late endosomes that carry HCV particles with the plasma membrane resulting in their release into the extracellular environment.[52] VTI1A is a SNARE involved in the vesicular transport from the late endosomes to the trans-Golgi network and forms a SNARE complex with STX16 and VAMP4 (Table S4).[54,55] STX8 is involved in the protein trafficking from the early to the late endosomes and exocytosis and forms a SNARE complex with STX7, VAMP8, and VTI1B.[55,56] A reduction in the expression of STX7, which interacts with both VTI1A and STX8 (Figure 2; Table S4), decreases HCV replication.[50] Taken together, the increased abundances of VTI1A and STX8 in CoreTGvsWT, but not PA28$\gamma^{-/-}$CoreTGvsWT, suggest potentially crucial roles of the two proteins in the HCV life cycle.

**PA28$\gamma^{-/-}$CoreTGvsCoreTG Extended Network.** Syntaxin 11 (STX11), a SNARE, was upregulated 3.52-fold in PA28$\gamma^{-/-}$CoreTGvsCoreTG (Table 1) and was mapped to the enriched KEGG Pathway "SNARE interactions in vesicular transport" ($p = 0.003$; Table S5). STX11 associates with the late endosomes and functions in the essential trafficking pathways (such as cytokine secretion) in the immune cells, with enhanced STX11 expression contributing to increased NK-cell mediated cytotoxicity.[57−61] STX11 binds with the SNARE VTI1B (Figure 3, Table S4) and regulates its participation the Q-SNARE complexes and, thus, the endocytic and exocytic trafficking in the macrophages. Overexpression of STX11 alters the VTI1B binding to STX6 and STX8 and likely reduces the endosomal transport to the cell surface.[57]

USO1, a Golgi-associated peripheral membrane protein, was decreased 2.05-fold in PA28$\gamma^{-/-}$CoreTGvsCoreTG (Table 1) and was identified as a significant linking component of the PA28$\gamma^{-/-}$CoreTGvsCoreTG SNARE network (Figure 3). USO1 plays an important role in ER to Golgi trafficking and its knockdown leads to the disintegration of the Golgi complex.[62,63] Decreased USO1 levels in PA28$\gamma^{-/-}$CoreTGvsCoreTG may, therefore, significantly impact the endosomal pathways associated with HCV release.

PA28$\gamma$ knockdown impairs the production of the infectious HCV particles (but not replication) in the JFH1 (HCV genotype 2a) infected cells, largely due to the deregulation of the E6AP-dependent Core degradation, which contributes to an antiviral response.[14] Our analysis suggests a potentially novel

**Table 2. Functional Analysis of the Extended Protein Interaction Networks[a]**

| proteins | data set[b] | KEGG pathways | prior involvement with HCV pathogenesis and HCC | probable associations with Core/PA28γ functions in HCV pathogenesis |
|---|---|---|---|---|
| AKT1 | I (−) | Insulin signaling pathway ($p = 5.72 \times 10^{-12}$) | reduced levels associated with insulin resistance (IR) in rats;[105] Akt phosphorylation is suppressed in the CoreTG mice and contributes to IR.[12] | Core-induced suppression of AKT1 levels may contribute to IR in HCV pathogenesis. |
| BAX | I (+) | Apoptosis ($p = 1.58 \times 10^{-18}$) | interacts with NS5A; disrupts mitochondrial homeostasis leading to abnormal cytochrome *c* release and apoptosis in HCV infection.[45,90,92,93] | Core-mediated BAX upregulation may induce host cell apoptosis. |
| CASP8 | I (+) | Apoptosis ($p = 1.58 \times 10^{-18}$) | activated in HCV infection.[90] | Core-mediated CASP8 upregulation may induce host cell apoptosis. |
| CDH1 | I (+) | Adherens junction ($p = 1.45 \times 10^{-20}$) | downregulated in the rat liver during hepatocarcinogenesis[106] | Core-mediated decrease in CDH1 levels may contribute to HCC |
| COMT | I (+); II (+) | Steroid hormone biosynthesis ($p = 0.002$) | upregulated in the lipid rafts in HCV infection;[50] COMT siRNA knockdown decreases HCV replication[103] | Core-induced activation of COMT may play an important role in HCV entry and replication |
| CSNK2B | II (+); III (+) | Adherens junction ($p = 1.4 \times 10^{-13}$); tight junction ($p = 4.46 \times 10^{-7}$) | interacts with the HCV NS3 protein;[45] regulates NS5A phosphorylation and hence infectious HCV particle production.[87] | loss of PA28γ activity may perturb CK2-mediated NS5A phosphorylation leading to decreased viral propagation. |
| EPS15 | I (+); III (−) | Endocytosis ($p = 2.08 \times 10^{-22}$) | elevated in human and mouse HCC;[107] mediates human enterovirus 71 entry via clathrin-mediated endocytosis,[108] which also mediates HCV internalization.[109] | elevated EPS15 levels may facilitate HCC; decreased EPS15 levels may contribute to the lack of HCC in the PA28$\gamma^{-/-}$CoreTG. May facilitate HCV entry via clathrin-mediated endocytosis. |
| MCM2 | I (+) | Cell cycle ($p = 1.82 \times 10^{-25}$) | increased hepatocyte MCM2 expression linked with fibrosis progression in HCV infection.[110] | Core-mediated enhanced MCM2 activity may contribute to fibrosis in HCV pathogenesis. |
| PTPN11 | II (+) | Natural killer cell mediated cytotoxicity ($p = 3.64 \times 10^{-10}$); Jak-STAT signaling pathway ($p = 5.74 \times 10^{-5}$) | functions as a tumor suppressor in HCC and negatively regulates hepatic insulin action.[111,112] | increased PTPN11 levels may be associated with the absence of HCC progression in PA28$\gamma^{-/-}$CoreTG. |
| RABEP1 | III (−) | Endocytosis ($p = 2.08 \times 10^{-22}$) | interacts with NS3;[45] functions in early endocytic events and regulates mast cell activation.[113,114] | may possibly function in HCV propagation. |
| RB1 | III (+) | Cell cycle ($p = 4.04 \times 10^{-20}$) | tumour suppressor, downregulated in HCC.[115,116] | increased RB1 levels in III consistent with the lack of HCC progression in the PA28$\gamma^{-/-}$CoreTG mice. |
| TRADD | III (−) | Apoptosis ($p = 1.84 \times 10^{-15}$) | forms a complex with Core and TNFR1, implicated in HCV-induced chronic liver disease.[117] | decreased TRADD levels may contribute to the lack of IR and liver disease in PA28$\gamma^{-/-}$CoreTG |

[a]Host factors that were previously known to be associated with HCV pathogenesis and HCC and were mapped to various enriched KEGG pathways associated with the CoreTGvsWT, PA28$\gamma^{-/-}$CoreTGvsWT, and PA28$\gamma^{-/-}$CoreTGvsCoreTG PPI networks. [b]Data set I: CoreTGvsWT; Data set II: PA28$\gamma^{-/-}$/CoreTGvsWT; Data set III: PA28$\gamma^{-/-}$/CoreTGvsCoreTG; +: upregulated; −: downregulated.



dx.doi.org/10.1021/pr300121a | J. Proteome Res. 2012, 11, 3664−3679

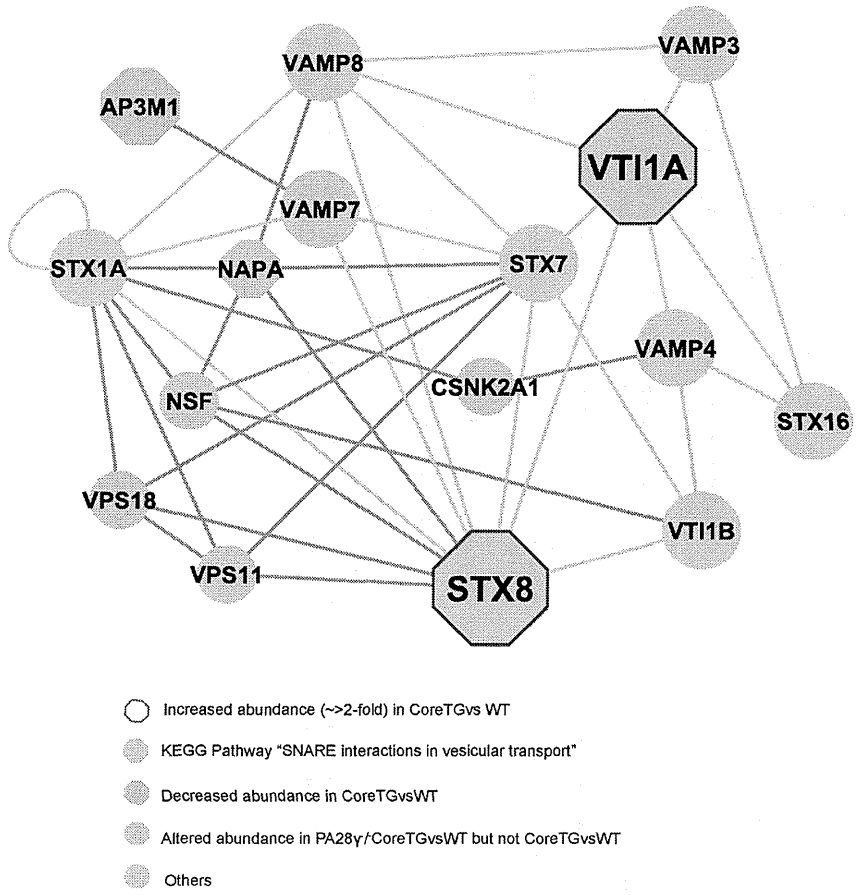


**Figure 2.** CoreTGvsWT SNARE network. Network illustration of the interactions between the PowerBlot identified differentially expressed proteins in CoreTGvsWT and human proteins mapped to the enriched KEGG pathway "SNARE interactions in vesicular transport". The node sizes differ for better clarity and do not reflect any topological attributes.

mechanism for the involvement of PA28$\gamma$ in HCV propagation. Potentially, the suppression of PA28$\gamma$ activity in PA28$\gamma^{-/-}$CoreTG mice may contribute to the overexpression of STX11 (and downregulation of USO1), thereby impairing the trafficking to the cell surface and consequently the release of the infectious HCV particles.

HCV has also been detected in the macrophages of certain infected patients,[64] suggesting that HCV may possibly infect the macrophages *in vivo* and regulate the STX11 (and USO1) expression to modulate the viral release and cytokine secretion.

EPS15 and RABEP1 (KEGG pathway "Endocytosis", $p = 2.08 \times 10^{-22}$) were decreased 2.11- and 2.74-fold, respectively, in PA28$\gamma^{-/-}$CoreTGvsCoreTG (Table 1, Table S5). EPS15 is an adaptor protein associated with the epidermal growth factor (EGF) signaling; it is localized to the clathrin-coated pits and functions in receptor-mediated endocytosis[65,66] and may play an important role in HCV pathogenesis (Table 2).

### Immune System and Signal Transduction

HCV infection induces varied active and passive host immune responses such as the recognition of the infecting HCV RNA and proteins by the macrophages and the dendritic cells expressing Toll-like receptors (TLRs) and RIG-I-like receptors (RLRs). These events trigger the production of Type I interferons (IFN-$\alpha/\beta$) and inflammatory cytokines in the infected hepatocytes, thereby initiating viral clearance. The ability to impair host immune responses contributes to the HCV persistence in the host.[67−72]

The PowerBlot analysis showed differentially expressed host proteins (IKBKG, MAP2K2, PPP3CA, SHC3, STAT1, TRADD) in PA28$\gamma^{-/-}$CoreTGvsCoreTG and their interacting partners that were mapped to one or more enriched KEGG pathways associated with the immune system (Table S5). IKBKG (IKK Gamma) is an antiapoptotic protein that is essential for NFKB activation and modulates TNF-mediated apoptosis.[73] IKBKG mutations are associated with immune deficiency phenotype (Table S7) and IKBKG may contribute to the activity of the hepatic carcinoma associated protein MAFIP in suppressing the proliferation of the cancer cells.[74] Additionally, specific deletion of IKBKG in the hepatocytes promotes NK-cell dependent liver damage.[75] Taken together, the elevated IKBKG abundance as observed in PA28$\gamma^{-/-}$CoreTGvsCoreTG (1.97-fold; Table 1) may contribute to the lack of HCC progression and reduced liver damage in the PA28$\gamma^{-/-}$CoreTG mice.

PPP3CA, MAP2K2, and SHC3 were mapped to the KEGG pathway "Natural killer cell mediated cytotoxicity" ($p = 1.67 \times 10^{-5}$; Table S5), the components of which function in the host immune response against the cancer cells and cells beset with pathogen infection.[76] PPP3CA levels were increased 12.94-fold,

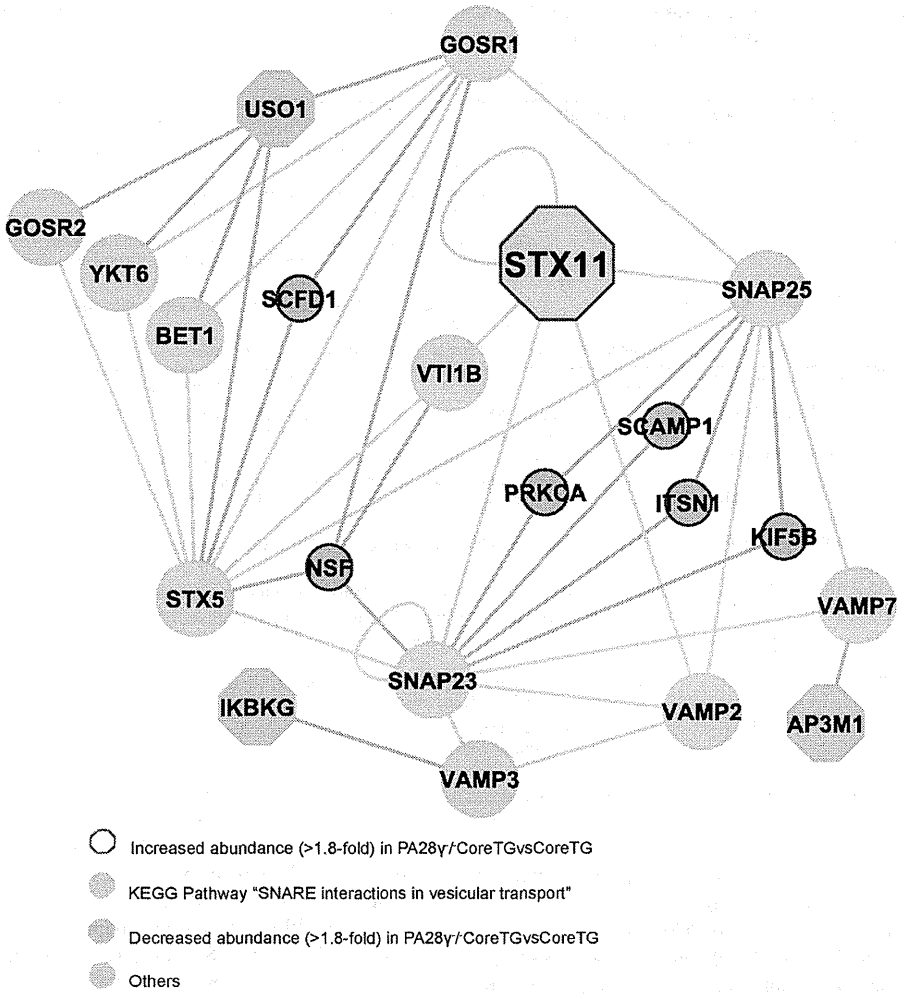


**Figure 3.** PA28$\gamma^{-}$/$^{-}$CoreTGvsCoreTG SNARE network. Network illustration of the interactions between the PowerBlot identified differentially expressed proteins in PA28$\gamma^{-}$/$^{-}$CoreTGvsCoreTG and human proteins mapped to the enriched KEGG pathway "SNARE interactions in vesicular transport". The node sizes differ for better clarity and do not reflect any topological attributes.

while MAP2K2 and SHC3 levels were suppressed 2.35-fold and 1.9-fold, respectively, in PA28$\gamma^{-/-}$CoreTGvsCoreTG (Table 1). These observations together with the increased STX11 abundance are consistent with the enhanced NK-cell mediated cytotoxicity that accompanies the STX11 overexpression.

PPP3CA is a tumor suppressor that negatively modulates the vascular endothelial growth factor (VEGF)-stimulated cell proliferation[77] and is downregulated in some cancerous cells.[78,79] PPP3CA was also mapped to the enriched KEGG pathways "VEGF signaling pathway" ($p = 2.59 \times 10^{-5}$), "MAPK signaling pathway" ($p = 2.37 \times 10^{-16}$) and "Wnt signaling pathway" ($p = 1.048 \times 10^{-10}$; Table S5), which are implicated in the HCV infection and HCC. The 7.55-fold increase in PPP3CA abundance in PA28$\gamma^{-/-}$CoreTGvsCoreTG (Table 1) suggests that increased PPP3CA activity may significantly contribute to the lack of tumorigenesis and HCC progression in PA28$\gamma^{-/-}$CoreTG mice.

MAP2PK2 is a dual specificity MAP kinase that plays a critical role in the mitogen growth factor signal transduction. It is a key regulator of the TNF-$\alpha$ signaling and plays an important role in the tumor progression in certain cancers.[80] Reduced MAP2K2 levels in the hepatocytes are implicated in enhanced apoptosis.[81] Therefore, the 2.66-fold decrease in MAP2K2 protein levels in PA28$\gamma^{-/-}$CoreTGvsCoreTG (Table 1) suggests that decreased MAP2K2 activity may contribute to the lack of HCC progression in PA28$\gamma^{-/-}$CoreTG mice. Our analysis thus identified potentially significant PA28$\gamma$-dependent roles of MAP2K2 and PPP3CA in a probable STX11-mediated regulation of NK cell activity in HCV pathogenesis.

MAP2K2, PPP3CA and SHC3 were also associated with the "Insulin signaling pathway" ($p = 5.88 \times 10^{-9}$; Table S5), the disruption of which may contribute to insulin resistance (IR). IR is linked with steatosis, fibrosis progression and poor interferon-$\alpha$ response in HCV infection.[82,83] PA28$\gamma$ contributes to hyperinsulinemia and IR in the CoreTG mice by impairing the insulin-signaling pathway through the suppression of Insulin receptor substrate 1 (IRS1) phosphorylation and increased tumor necrosis factor alpha (TNF-$\alpha$) secretion.[12,84] The Powerblot analysis revealed that TRADD, which regulates TNF-$\alpha$ signaling as an antiapoptotic factor[85,86] and possibly functions in HCV pathogenesis (Table 2), was suppressed 2-fold in PA28$\gamma^{-/-}$CoreTGvsWT (Table 1).

**Table 3. Summary of Proteins and Pathways Prioritized with TargetMine and Adjusted with the Help of Knowledge-Based Inputs for Experimental Investigation and/or Biomarker Discovery**

(a) HCV replication and release

| KEGG pathways | *p*-value | proteins[a] | data set[b] | knowledge-based evidence | refs |
|---|---|---|---|---|---|
| SNARE interactions in vesicular transport | 0.023 | VTI1A (+), STX8 (+) | I | regulation of the endosome-based membrane trafficking pathway implicated in HCV release | 50, 52, 55 |
| Steroid hormone biosynthesis | 0.002 | COMT (+) | I | COMT siRNA impairs HCV genotype 1b replication; functions in genotype 2a replication not known | 50, 103 |
| SNARE interactions in vesicular transport | 0.003 | STX11 (+) | III | modulation of specific components of the endosome-based membrane trafficking pathway implicated in HCV release; modulation of cytokine secretion in immune cells | 50, 55, 57 |
| Endocytosis | $1.03 \times 10^{-18}$ | CAV1 (+) | I | close homologue CAV2 associated with HCV replication complex; possible role in HCV replication | 103 |

(b) steatosis, fibrosis, and hepatcarcinogenesis in HCV infection

| KEGG pathways | *p*-value | proteins[a] | data set[b] | knowledge-based evidence | refs |
|---|---|---|---|---|---|
| Insulin signaling pathway | $5.72 \times 10^{-12}$ | AKT1 (−) | I | reduced AKT1 levels and phosophorylation associated with insulin resistance, which contributes to steatosis, fibrosis and HCC | 118 |
| Natural killer cell mediated cytotoxicity | $1.67 \times 10^{-5}$ | PPP3CA (+), MAP2K2 (−) | III | PPP3CA is a tumor suppressor with decreased levels in some cancers; PTPN1 is a tumor suppressor and regulates hepatic insulin signaling; decreased MAP2K2 levels in hepatocytes associated with enhanced apoptosis | 78, 79, 81 |
| Adherens junction | $1.45 \times 10^{-20}$ | CDH1 (−) | I | decreased CDH1 abundance associated with hepatocarcinogenesis and various cancers | 106 |
| Focal adhesion | $5.57 \times 10^{-12}$ | SHC1 (+) | II | loss of SHC1 function associated with tumor metastasis | 119 |
| Apoptosis | $1.58 \times 10^{-18}$ | BAX (+), CASP8 (+) | I | BAX interacts with NS5A and contributes to abnormal cytochrome *c* release in HCV infection; CASP8 activated in HCV infection | 45, 90, 92, 93 |
| Apoptosis | $1.84 \times 10^{-15}$ | TRADD (−) | III | antiapoptotic factor that forms a ternary complex containing Core, with likely functions in HCV-induced chronic liver disease | 117 |
| Chemokine signaling pathway | $1.18 \times 10^{-13}$ | ARRB1 (−) | I | interacts with PKM2, a key enzyme in glycolytic metabolism and cell growth and death in tumor cells | 120 |

[a]+: upregulated. −: downregulated. [b]Data set I: CoreTGvsWT; Data set II: PA28$\gamma^{-/-}$/CoreTGvsWT; Data set III: PA28$\gamma^{-/-}$/CoreTGvsCoreTG.

### Cell Adhesion

The Powerblot analysis revealed that host protein CSNK2B, the regulatory (beta) subunit of Casein Kinase II (CK2), was increased 1.88-fold in PA28$\gamma^{-/-}$CoreTGvsCoreTG (1.9-fold in PA28$\gamma^{-/-}$CoreTGvsWT). CK2 phosphorylates NS5A and regulates the production of infectious viral particles[87] and thus HCV pathogenesis (Table 2). CSNK2B was mapped to the enriched KEGG pathways "Adherens junction" ($p = 1.4 \times 10^{-13}$) and "Tight junction" ($p = 4.46 \times 10^{-7}$), some components of which are implicated in HCV entry and infection.[88]

SHC3 and TNR were decreased 1.9- and 4.62-fold, respectively, in PA28$\gamma^{-/-}$CoreTGvsCoreTG and were mapped to the enriched KEGG pathway "Focal adhesion" ($p = 3.56 \times 10^{-12}$; Table 1; Table S5), which regulates cell migration and adhesion to the extracellular matrix. Its deregulation is linked with tumor progression and possibly HCV propagation.[45] Previously, a Core interacting protein ENO1, associated with the focal adhesion, was identified as a novel regulator of HCV replication and release,[22] suggesting that SHC3 and TNR may play important roles in HCV pathogenesis.

### Cell Growth and Death

Host cell apoptosis plays a critical role in HCV pathogenesis. The induction of apoptosis in the hepatocytes contributes to cell damage and fibrosis, whereas the induction of apoptosis in the peripheral blood mononuclear cells (PMBC), such as the T-cells, contributes significantly to the impaired immune response and HCV persistence in the host.[89−94] PA28$\gamma$ is implicated in the cell cycle regulation, cell proliferation, and apoptosis[95−98] and likely plays a critical role in the manipulation of the cell cycle and apoptosis in HCV pathogenesis.

PPP3CA, TRADD, PRKAR2A, and IKBKG, with increased or decreased abundances in PA28$\gamma^{-/-}$CoreTGvsCoreTG, were mapped to KEGG pathway "Apoptosis" ($p = 1.84 \times 10^{-15}$; Table S5). PPP3CA was also mapped to "Oocyte meiosis" ($p = 9.84 \times 10^{-10}$; Table S5), associated with cell division. PPP3CA levels were highly elevated (12.94-fold) in PA28$\gamma^{-/-}$CoreTGvsCoreTG (Table 1), which may contribute to the accelerated cell death and the lack of tumor progression in PA28$\gamma^{-/-}$CoreTG mice.

PRKAR2A levels were decreased 1.88-fold in PA28$\gamma^{-/-}$CoreTGvsCoreTG (Table 1). PRKAR2A codes for a regulatory subunit of the cAMP dependent protein kinase (PKA), an important mediator of the cAMP signal transduction and elevated PRKAR2A expression is associated with an increased proliferation of the rat alveolar cells.[99] The suppression of PRKAR2A activity may therefore contribute to the lack of tumor proliferation in the PA28$\gamma^{-/-}$CoreTG mice.

### Prioritization and Validation of the Novel Candidates for Their Role in HCV Replication and Release

Target prioritiszation using TargetMine is a simple process that involves uploading an initial list of candidates (in this instance the proteins in the CoreTGvsWT, PA28$\gamma^{-/-}$CoreTGvsWT, and PA28$\gamma^{-/-}$CoreTGvsCoreTG extended PPI networks) and estimating enriched biological themes associated with the input list.[16] Knowledge-based inputs may then be employed to further screen the proteins mapped to the top ranking significant associations to infer a manageable set of candidates. With the help of TargetMine, we previously investigated the significance of interactions between HCV Core and NS4B proteins and host factors in HCV infection and identified three novel regulators of HCV replication and propagation.[22]


dx.doi.org/10.1021/pr300121a | J. Proteome Res. 2012, 11, 3664−3679

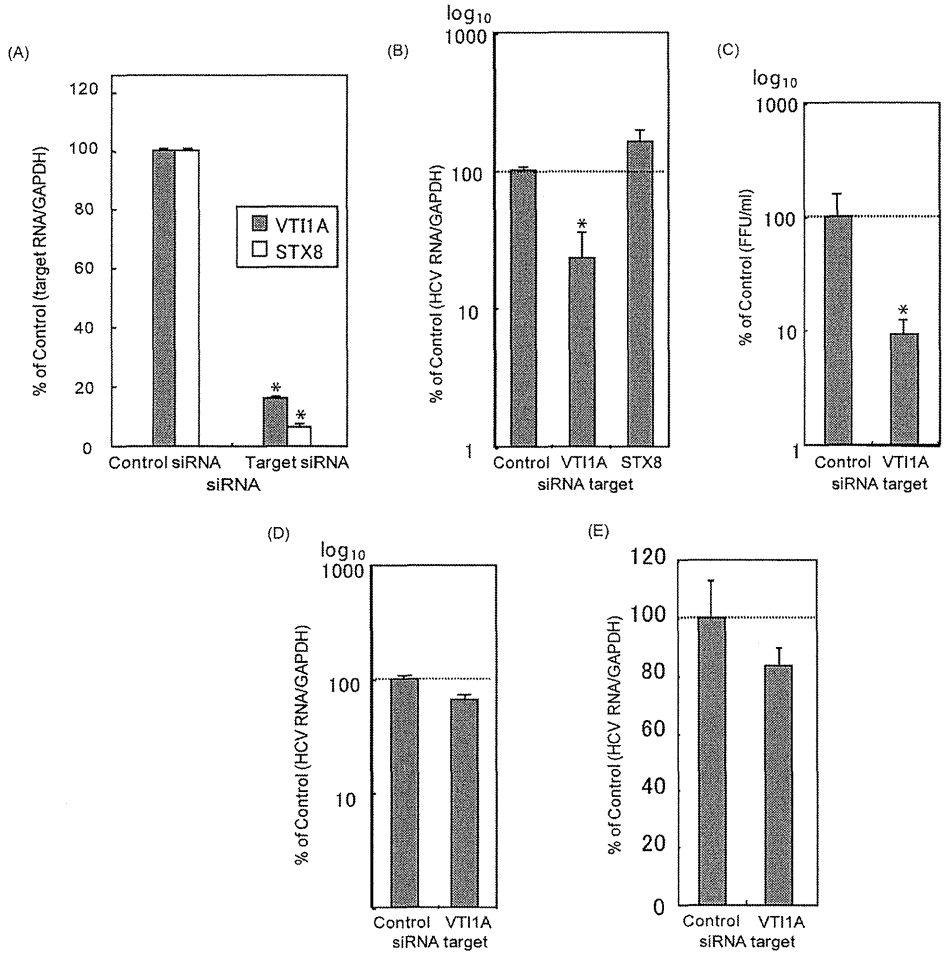


**Figure 4.** Effects of knockdown of candidate proteins on HCV propagation and replication. Host proteins VTI1A and STX8 were suppressed by RNAi (A) in Huh7OK1 cells infected with HCV JFH1 strain (genotype 2a; B, C, D) and in cells including subgenomic JFH1 replicon (E). The amounts of mRNA of the intracellular host proteins (A) and the supernatant viral RNA (B), viral titer (C), and intracellular viral RNA were estimated (D). The amount of the subgenomic viral RNA was also estimated (E). Each value was represented as percentage of the cells transfected with control siRNA; FFU: focus-forming units; * $p < 0.01$.

Table 3 summarizes the prioritized candidates and pathways, all of which have been discussed above. Traditionally, viral and host proteins associated with the HCV lifecycle (internalization, replication, assembly, and release) have been preferred targets in the anti-HCV studies. The prioritized candidates and pathways in Table 3a fall within this category. In particular, our analysis suggested novel and potentially crucial roles of the host proteins VTI1A and STX8, which were elevated in CoreTG but not in PA28$\gamma^{-/-}$CoreTG, in the replication and/or the release stages of the HCV lifecycle, therefore making these host proteins attractive targets for further investigation.

Because of the lack of a suitable model system for HCV infection, cell-culture-based systems for HCV RNA replication and infectious viral particle production have been extensively exploited to identify potential anti-HCV drug targets.[5,7−9] To further explore the roles of selected candidates in the HCV life cycle, we performed cellular assays to assess the impact of VTI1A and STX8 siRNA knockdowns on HCV replication and release. Since the HCV-production systems using the HCV JFH1 infectious strain (genotype 2a) isolates alone are capable of both efficient replication and the production of the infectious HCV particles,[33,100] JFH1 was used to infect the Huh7OK1 cell line 24 h after transfection with each siRNA (see Materials and Methods). The infected cells were harvested after 72 h post-infection and the expression of each host protein was assessed by qRT-PCR (Figure 4A). Supernatant viral RNA and the viral titer were significantly decreased by the knockdown of VTI1A but were unaffected by the STX8 knockdown (Figure 4B,C). However, VTI1A and STX8A knockdowns had no effect on the intracellular viral RNA levels in the HCV infected cells (Figure 4D) or replicon cells derived from JFH1 strain (Figure 4E) or replicon cells derived from the Con1 (genotype 1b) strain (data not shown). These observations suggest that VTI1A regulates HCV propagation but not HCV replication.

The standard therapy of PEGylated interferon-$\alpha$ plus rebavirin treatment often results in severe side effects such as depression, flu-like symptoms, anemia, and fatigue that force the treatment to discontinue in affected patients, thus necessitating improved and combinatorial treatment strategies.[101,102] The genetic variability of HCV has led to increasing drug resistance. Thus, antivirals that target host proteins critical to viral pathogenesis, with a lower rate of mutation and


dx.doi.org/10.1021/pr300121a | J. Proteome Res. 2012, 11, 3664−3679

preferably with minimal adverse side effects, may provide attractive alternatives to HCV protein targets. VTI1A-deficient (knockout) mice are viable and fertile,[55] suggesting that the suppression of VTI1A activity may not have significantly undesirable side effects.

Inhibition of COMT (which was increased 2.71- and 2.96-fold in CoreTGvsWT and PA28$\gamma^{-/-}$CoreTG, respectively; Table 1) activity via siRNA knockdown was previously shown to result in a decreased HCV replication in cells infected with the Con1 strain.[103] To investigate other possible aspects (such as genotype specificity) of COMT function in the HCV life cycle, we assessed the impact of the COMT siRNA knockdown on HCV replication and release. COMT knockdown, however, had no effect on HCV propagation or replication in the cells including full length or subgenomic replicons derived from JFH1 or Con1 strains (data not shown). The discrepancy between our observations and those of Chan et al.[103] may be explained by the differences in the methodologies. We employed a transient transfection method to knockdown the selected targets to assess their roles in HCV replication and release, whereas Chan et al. employed a lentiviral expressing system for their experiments. Lentiviral mediated siRNA delivery is known to result in a persistent knockdown of gene expression,[104] and a persistent knockdown of COMT expression may be necessary to inhibit HCV replication *in vitro*.

That we were able to experimentally validate one of the three genes selected for experimental characterization reinforces the strengths of the elaborate PPI network-based approach to identify and prioritize suitable targets for experimental and therapeutic investigation.

## CONCLUSIONS

By analyzing high-throughput proteomics data from transgenic mice expressing HCV Core protein in the liver (an *in vivo* model of HCV pathogenesis) with or without the knockout of the proteasome activator PA28$\gamma$, we highlighted the cellular responses to HCV infection *in vivo* and obtained further insights into the role of PA28$\gamma$ in HCV infection.

We investigated the network context of the changes in the protein abundances by mapping them onto the human interactome with the help of the TargetMine data warehouse. The differentially expressed proteins that were integrated with the human interactome were observed to participate in compact and well connected cellular networks reflecting the ability of HCV to rapidly and efficiently react to the host responses to HCV infection. A functional analysis of the PPI networks highlighted the cellular pathways associated with vesicular transport, immune system, cellular adhesion, cell growth, and cell death among others that were most prominently influenced by Core and PA28$\gamma$ in HCV infection. We also confirmed the previous observations that host factors such as AKT1, BAX, CASP8 CDH1, COMT, MCM2, PTPN11, and RB1 showed increased or decreased abundances in HCV infection. However, to the best of our knowledge, the precise molecular mechanisms of these factors' involvement in HCV pathogenesis and HCC were unknown, and our analysis suggests novel contributions of Core and PA28$\gamma$ to the functions of these proteins.

Our observations were then used to prioritize potential candidates for the follow-up experimental investigations. Cellular assays based on siRNA knockdowns of selected candidates in the HCV infected and replicon cells validated VTI1A, a SNARE protein associated with vesicular transport, which was upregulated in CoreTG but not in PA28$\gamma^{-/-}$CoreTG, as a novel regulator of HCV propagation but not replication. VTIA-deficient mice are largely indistinguishable from the normal mice except for minor growth retardation in a few instances; therefore, VTI1A is a promising novel candidate for anti-HCV therapy.

Our analysis not only builds on the present understanding of the Core-PA28$\gamma$ interplay in HCV infection but also provides novel insights that would facilitate the clinical evaluation of proteomic changes associated with HCV pathogenesis. Our analysis also provides a generic framework for investigating large scale proteomic data. Such investigation may help identify common themes associated with different physiological conditions, especially pathogen (such as viral) infection and disease, and help develop effective broad spectrum strategies aimed at ameliorating pathogen infection and diseases.

## ASSOCIATED CONTENT

### Supporting Information

This material is available free of charge via the Internet at http://pubs.acs.org.

## AUTHOR INFORMATION


### Corresponding Author

*Tel: +81-72-641-9890. Fax: +81-72-641-9881. E-mail: kenji@nibio.go.jp.

### Author Contributions

‖These authors contributed equally to this work.


### Notes

The authors declare no competing financial interest.

## ACKNOWLEDGMENTS

This study was supported by the Industrial Technology Research Grant Program in 2007 from New Energy and Industrial Technology Development Organization (NEDO) of Japan and also by grants-in-aid from the Ministry of Health, Labor, and Welfare; the Ministry of Education, Culture, Sports, Science, and Technology; the Osaka University Global Center of Excellence Program; and the Foundation for Biomedical Research and Innovation. We gratefully acknowledge Dr. T. Wakita for providing us with cell lines and plasmids.

## REFERENCES


(1) Dubuisson, J. Hepatitis C virus proteins. *World J. Gastroenterol.* **2007**, *13* (17), 2406–15.

(2) Moriishi, K.; Mochizuki, R.; Moriya, K.; Miyamoto, H.; Mori, Y.; Abe, T.; Murata, S.; Tanaka, K.; Miyamura, T.; Suzuki, T.; Koike, K.; Matsuura, Y. Critical role of PA28gamma in hepatitis C virus-associated steatogenesis and hepatocarcinogenesis. *Proc. Natl. Acad. Sci. U.S.A.* **2007**, *104* (5), 1661–6.

(3) Myrmel, H.; Ulvestad, E.; Asjo, B. The hepatitis C virus enigma. *APMIS* **2009**, *117* (5–6), 427–39.

(4) Tang, H.; Grise, H. Cellular and molecular biology of HCV infection and hepatitis. *Clin. Sci. (London)* **2009**, *117* (2), 49–65.

(5) Moradpour, D.; Penin, F.; Rice, C. M. Replication of hepatitis C virus. *Nat. Rev. Microbiol.* **2007**, *5* (6), 453–63.

(6) Simmonds, P.; Bukh, J.; Combet, C.; Deleage, G.; Enomoto, N.; Feinstone, S.; Halfon, P.; Inchauspe, G.; Kuiken, C.; Maertens, G.; Mizokami, M.; Murphy, D. G.; Okamoto, H.; Pawlotsky, J. M.; Penin, F.; Sablon, E.; Shin, I. T.; Stuyver, L. J.; Thiel, H. J.; Viazov, S.; Weiner, A. J.; Widell, A. Consensus proposals for a unified system of nomenclature of hepatitis C virus genotypes. *Hepatology* **2005**, *42* (4), 962–73.

(7) De Francesco, R.; Migliaccio, G. Challenges and successes in developing new therapies for hepatitis C. *Nature* **2005**, *436* (7053), 953–60.
(8) Kato, N.; Mori, K.; Abe, K.; Dansako, H.; Kuroki, M.; Ariumi, Y.; Wakita, T.; Ikeda, M. Efficient replication systems for hepatitis C virus using a new human hepatoma cell line. *Virus Res.* **2009**, *146* (1–2), 41–50.
(9) Murray, C. L.; Rice, C. M. Hepatitis C: An unsuspected drug target. *Nature* **2010**, *465* (7294), 42–4.
(10) Mori, Y.; Moriishi, K.; Matsuura, Y. Hepatitis C virus core protein: its coordinate roles with PA28gamma in metabolic abnormality and carcinogenicity in the liver. *Int. J. Biochem. Cell Biol.* **2008**, *40* (8), 1437–42.
(11) Gao, G.; Luo, H. The ubiquitin-proteasome pathway in viral infections. *Can. J. Physiol. Pharmacol.* **2006**, *84* (1), 5–14.
(12) Miyamoto, H.; Moriishi, K.; Moriya, K.; Murata, S.; Tanaka, K.; Suzuki, T.; Miyamura, T.; Koike, K.; Matsuura, Y. Involvement of the PA28gamma-dependent pathway in insulin resistance induced by hepatitis C virus core protein. *J. Virol.* **2007**, *81* (4), 1727–35.
(13) Moriishi, K.; Okabayashi, T.; Nakai, K.; Moriya, K.; Koike, K.; Murata, S.; Chiba, T.; Tanaka, K.; Suzuki, R.; Suzuki, T.; Miyamura, T.; Matsuura, Y. Proteasome activator PA28gamma-dependent nuclear retention and degradation of hepatitis C virus core protein. *J. Virol.* **2003**, *77* (19), 10237–49.
(14) Moriishi, K.; Shoji, I.; Mori, Y.; Suzuki, R.; Suzuki, T.; Kataoka, C.; Matsuura, Y. Involvement of PA28gamma in the propagation of hepatitis C virus. *Hepatology* **2010**, *52* (2), 411–20.
(15) Suzuki, R.; Moriishi, K.; Fukuda, K.; Shirakura, M.; Ishii, K.; Shoji, I.; Wakita, T.; Miyamura, T.; Matsuura, Y.; Suzuki, T. Proteasomal turnover of hepatitis C virus core protein is regulated by two distinct mechanisms: a ubiquitin-dependent mechanism and a ubiquitin-independent but PA28gamma-dependent mechanism. *J. Virol.* **2009**, *83* (5), 2389–92.
(16) Chen, Y. A.; Tripathi, L. P.; Mizuguchi, K. TargetMine, an integrated data warehouse for candidate gene prioritisation and target discovery. *PLoS One* **2011**, *6* (3), e17844.
(17) Liu, M. C.; Akle, V.; Zheng, W.; Dave, J. R.; Tortella, F. C.; Hayes, R. L.; Wang, K. K. Comparing calpain- and caspase-3-mediated degradation patterns in traumatic brain injury by differential proteome analysis. *Biochem. J.* **2006**, *394* (Pt 3), 715–25.
(18) Stark, C.; Breitkreutz, B. J.; Reguly, T.; Boucher, L.; Breitkreutz, A.; Tyers, M. BioGRID: a general repository for interaction datasets. *Nucleic Acids Res.* **2006**, *34* (Database issue), D535–9.
(19) Turner, B.; Razick, S.; Turinsky, A. L.; Vlasblom, J.; Crowdy, E. K.; Cho, E.; Morrison, K.; Donaldson, I. M.; Wodak, S. J. iRefWeb: interactive analysis of consolidated protein interaction data and their supporting evidence. *Database (Oxford)* **2010**, *2010*, baq023.
(20) Cline, M. S.; Smoot, M.; Cerami, E.; Kuchinsky, A.; Landys, N.; Workman, C.; Christmas, R.; Avila-Campilo, I.; Creech, M.; Gross, B.; Hanspers, K.; Isserlin, R.; Kelley, R.; Killcoyne, S.; Lotia, S.; Maere, S.; Morris, J.; Ono, K.; Pavlovic, V.; Pico, A. R.; Vailaya, A.; Wang, P. L.; Adler, A.; Conklin, B. R.; Hood, L.; Kuiper, M.; Sander, C.; Schmulevich, I.; Schwikowski, B.; Warner, G. J.; Ideker, T.; Bader, G. D. Integration of biological networks and gene expression data using Cytoscape. *Nat. Protoc.* **2007**, *2* (10), 2366–82.
(21) Assenov, Y.; Ramirez, F.; Schelhorn, S. E.; Lengauer, T.; Albrecht, M. Computing topological parameters of biological networks. *Bioinformatics* **2008**, *24* (2), 282–4.
(22) Tripathi, L. P.; Kataoka, C.; Taguwa, S.; Moriishi, K.; Mori, Y.; Matsuura, Y.; Mizuguchi, K. Network based analysis of hepatitis C virus Core and NS4B protein interactions. *Mol. Biosyst.* **2010**, *6* (12), 2539–53.
(23) Ashburner, M.; Ball, C. A.; Blake, J. A.; Botstein, D.; Butler, H.; Cherry, J. M.; Davis, A. P.; Dolinski, K.; Dwight, S. S.; Eppig, J. T.; Harris, M. A.; Hill, D. P.; Issel-Tarver, L.; Kasarskis, A.; Lewis, S.; Matese, J. C.; Richardson, J. E.; Ringwald, M.; Rubin, G. M.; Sherlock, G. Gene ontology: tool for the unification of biology. The Gene Ontology Consortium. *Nat. Genet.* **2000**, *25* (1), 25–9.
(24) Aoki-Kinoshita, K. F.; Kanehisa, M. Gene annotation and pathway mapping in KEGG. *Methods Mol. Biol.* **2007**, *396*, 71–91.
(25) McKusick-Nathans Institute of Genetic Medicine, Johns Hopkins Medicine (Baltimore, MD) and National Center for Biotechnology Information, National Library of Medicine (Bethesda, MD), Online Mendelian Inheritance in Man, OMIM (TM). In 2010.
(26) Benjamini, Y.; Hochberg, Y. Controlling the false discovery rate-A practical and powerful approach to multiple testing. *J. R. Statist. Soc. B* **1995**, *57* (1), 289–300.
(27) Noble, W. S. How does multiple testing correction work? *Nat. Biotechnol.* **2009**, *27* (12), 1135–7.
(28) Linhart, C.; Halperin, Y.; Shamir, R. Transcription factor and microRNA motif discovery: the Amadeus platform and a compendium of metazoan target sets. *Genome Res.* **2008**, *18* (7), 1180–9.
(29) Montgomery, S. B.; Griffith, O. L.; Sleumer, M. C.; Bergman, C. M.; Bilenky, M.; Pleasance, E. D.; Prychyna, Y.; Zhang, X.; Jones, S. J. ORegAnno: an open access database and curation system for literature-derived promoters, transcription factor binding sites and regulatory variation. *Bioinformatics* **2006**, *22* (5), 637–40.
(30) Okamoto, T.; Omori, H.; Kaname, Y.; Abe, T.; Nishimura, Y.; Suzuki, T.; Miyamura, T.; Yoshimori, T.; Moriishi, K.; Matsuura, Y. A single-amino-acid mutation in hepatitis C virus NS5A disrupting FKBP8 interaction impairs viral replication. *J. Virol.* **2008**, *82* (7), 3480–9.
(31) Pietschmann, T.; Lohmann, V.; Kaul, A.; Krieger, N.; Rinck, G.; Rutter, G.; Strand, D.; Bartenschlager, R. Persistent and transient replication of full-length hepatitis C virus genomes in cell culture. *J. Virol.* **2002**, *76* (8), 4008–21.
(32) Kato, T.; Date, T.; Miyamoto, M.; Furusaka, A.; Tokushige, K.; Mizokami, M.; Wakita, T. Efficient replication of the genotype 2a hepatitis C virus subgenomic replicon. *Gastroenterology* **2003**, *125* (6), 1808–17.
(33) Wakita, T.; Pietschmann, T.; Kato, T.; Date, T.; Miyamoto, M.; Zhao, Z.; Murthy, K.; Habermann, A.; Krausslich, H. G.; Mizokami, M.; Bartenschlager, R.; Liang, T. J. Production of infectious hepatitis C virus in tissue culture from a cloned viral genome. *Nat. Med.* **2005**, *11* (7), 791–6.
(34) Cao, W.; Sun, B.; Feitelson, M. A.; Wu, T.; Tur-Kaspa, R.; Fan, Q. Hepatitis C virus targets over-expression of arginase I in hepatocarcinogenesis. *Int. J. Cancer* **2009**, *124* (12), 2886–92.
(35) Tacke, R. S.; Tosello-Trampont, A.; Nguyen, V.; Mullins, D. W.; Hahn, Y. S. Extracellular hepatitis C virus core protein activates STAT3 in human monocyte/macrophage/dendritic cells via an IL-6 autocrine pathway. *J. Biol. Chem.* **2011**, DOI: 10.1074/jbc.M110.217653 .
(36) Waris, G.; Turkson, J.; Hassanein, T.; Siddiqui, A. Hepatitis C virus (HCV) constitutively activates STAT-3 via oxidative stress: role of STAT-3 in HCV replication. *J. Virol.* **2005**, *79* (3), 1569–80.
(37) Randall, G.; Panis, M.; Cooper, J. D.; Tellinghuisen, T. L.; Sukhodolets, K. E.; Pfeffer, S.; Landthaler, M.; Landgraf, P.; Kan, S.; Lindenbach, B. D.; Chien, M.; Weir, D. B.; Russo, J. J.; Ju, J.; Brownstein, M. J.; Sheridan, R.; Sander, C.; Zavolan, M.; Tuschl, T.; Rice, C. M. Cellular cofactors affecting hepatitis C virus infection and replication. *Proc. Natl. Acad. Sci. U.S.A.* **2007**, *104* (31), 12884–9.
(38) Lin, W.; Kim, S. S.; Yeung, E.; Kamegaya, Y.; Blackard, J. T.; Kim, K. A.; Holtzman, M. J.; Chung, R. T. Hepatitis C virus core protein blocks interferon signaling by interaction with the STAT1 SH2 domain. *J. Virol.* **2006**, *80* (18), 9226–35.
(39) Tsutsumi, T.; Suzuki, T.; Moriya, K.; Shintani, Y.; Fujie, H.; Miyoshi, H.; Matsuura, Y.; Koike, K.; Miyamura, T. Hepatitis C virus core protein activates ERK and p38 MAPK in cooperation with ethanol in transgenic mice. *Hepatology* **2003**, *38* (4), 820–8.
(40) Nanda, S. K.; Herion, D.; Liang, T. J. The SH3 binding motif of HCV [corrected] NS5A protein interacts with Bin1 and is important for apoptosis and infectivity. *Gastroenterology* **2006**, *130* (3), 794–809.
(41) Jacobs, J. M.; Diamond, D. L.; Chan, E. Y.; Gritsenko, M. A.; Qian, W.; Stastna, M.; Baas, T.; Camp, D. G., 2nd; Carithers, R. L., Jr.; Smith, R. D.; Katze, M. G. Proteome analysis of liver cells expressing a full-length hepatitis C virus (HCV) replicon and biopsy specimens of

posttransplantation liver from HCV-infected patients. *J. Virol.* **2005**, *79* (12), 7558–69.
(42) Woodhouse, S. D.; Narayan, R.; Latham, S.; Lee, S.; Antrobus, R.; Gangadharan, B.; Luo, S.; Schroth, G. P.; Klenerman, P.; Zitzmann, N. Transcriptome sequencing, microarray, and proteomic analyses reveal cellular and metabolic impact of hepatitis C virus infection in vitro. *Hepatology* **2010**, *52* (2), 443–53.
(43) Fujino, T.; Nakamuta, M.; Yada, R.; Aoyagi, Y.; Yasutake, K.; Kohjima, M.; Fukuizumi, K.; Yoshimoto, T.; Harada, N.; Yada, M.; Kato, M.; Kotoh, K.; Taketomi, A.; Maehara, Y.; Nakashima, M.; Enjoji, M. Expression profile of lipid metabolism-associated genes in hepatitis C virus-infected human liver. *Hepatol. Res.* **2010**, *40* (9), 923–9.
(44) MacPherson, J. I.; Sidders, B.; Wieland, S.; Zhong, J.; Targett-Adams, P.; Lohmann, V.; Backes, P.; Delpuech-Adams, O.; Chisari, F.; Lewis, M.; Parkinson, T.; Robertson, D. L. An integrated transcriptomic and meta-analysis of hepatoma cells reveals factors that influence susceptibility to HCV infection. *PLoS One* **2011**, *6* (10), e25584.
(45) de Chassey, B.; Navratil, V.; Tafforeau, L.; Hiet, M. S.; Aublin-Gex, A.; Agaugue, S.; Meiffren, G.; Pradezynski, F.; Faria, B. F.; Chantier, T.; Le Breton, M.; Pellet, J.; Davoust, N.; Mangeot, P. E.; Chaboud, A.; Penin, F.; Jacob, Y.; Vidalain, P. O.; Vidal, M.; Andre, P.; Rabourdin-Combe, C.; Lotteau, V. Hepatitis C virus infection protein network. *Mol. Syst. Biol.* **2008**, *4*, 230.
(46) Chazal, N.; Gerlier, D. Virus entry, assembly, budding, and membrane rafts. *Microbiol. Mol. Biol. Rev.* **2003**, *67* (2), 226–37.
(47) Manes, S.; del Real, G.; Martinez, A. C. Pathogens: raft hijackers. *Nat. Rev. Immunol.* **2003**, *3* (7), 557–68.
(48) Riethmuller, J.; Riehle, A.; Grassme, H.; Gulbins, E. Membrane rafts in host-pathogen interactions. *Biochim. Biophys. Acta* **2006**, *1758* (12), 2139–47.
(49) Suzuki, T.; Suzuki, Y. Virus infection and lipid rafts. *Biol. Pharm. Bull.* **2006**, *29* (8), 1538–41.
(50) Mannova, P.; Fang, R.; Wang, H.; Deng, B.; McIntosh, M. W.; Hanash, S. M.; Beretta, L. Modification of host lipid raft proteome upon hepatitis C virus replication. *Mol. Cell. Proteomics* **2006**, *5* (12), 2319–25.
(51) Corless, L.; Crump, C. M.; Griffin, S. D.; Harris, M. Vps4 and the ESCRT-III complex are required for the release of infectious hepatitis C virus particles. *J. Gen. Virol.* **2010**, *91* (Pt 2), 362–72.
(52) Lai, C. K.; Jeng, K. S.; Machida, K.; Lai, M. M. Hepatitis C virus egress and release depend on endosomal trafficking of core protein. *J. Virol.* **2010**, *84* (21), 11590–8.
(53) Jahn, R.; Scheller, R. H. SNAREs—engines for membrane fusion. *Nat. Rev. Mol. Cell. Biol.* **2006**, *7* (9), 631–43.
(54) Kreykenbohm, V.; Wenzel, D.; Antonin, W.; Atlachkine, V.; von Mollard, G. F. The SNAREs vti1a and vti1b have distinct localization and SNARE complex partners. *Eur. J. Cell Biol.* **2002**, *81* (5), 273–80.
(55) Kunwar, A. J.; Rickmann, M.; Backofen, B.; Browski, S. M.; Rosenbusch, J.; Schoning, S.; Fleischmann, T.; Krieglstein, K.; Fischer von Mollard, G. Lack of the endosomal SNAREs vti1a and vti1b led to significant impairments in neuronal development. *Proc. Natl. Acad. Sci. U.S.A.* **2011**, *108* (6), 2575–80.
(56) Mascia, L.; Langosch, D. Evidence that late-endosomal SNARE multimerization complex is promoted by transmembrane segments. *Biochim. Biophys. Acta* **2007**, *1768* (3), 457–66.
(57) Offenhauser, C.; Lei, N.; Roy, S.; Collins, B. M.; Stow, J. L.; Murray, R. Z. Syntaxin 11 binds Vti1b and regulates late endosome to lysosome fusion in macrophages. *Traffic* **2011**, *12*, 762–73.
(58) Bryceson, Y. T.; Chiang, S. C.; Darmanin, S.; Fauriat, C.; Schlums, H.; Theorell, J.; Wood, S. M. Molecular mechanisms of natural killer cell activation. *J. Innate Immun.* **2011**, *3* (3), 216–26.
(59) Arneson, L. N.; Brickshawana, A.; Segovis, C. M.; Schoon, R. A.; Dick, C. J.; Leibson, P. J. Cutting edge: syntaxin 11 regulates lymphocyte-mediated secretion and cytotoxicity. *J. Immunol.* **2007**, *179* (6), 3397–401.
(60) Dabrazhynetskaya, A.; Ma, J.; Guerreiro-Cacais, A. O.; Arany, Z.; Rudd, E.; Henter, J. I.; Karre, K.; Levitskaya, J.; Levitsky, V. Syntaxin 11 marks a distinct intracellular compartment recruited to the immunological synapse of NK cells to co-localize with cytotoxic granules. *J. Cell. Mol. Med.* **2011**, *16*, 129–41.
(61) Gholam, C.; Grigoriadou, S.; Gilmour, K. C.; Gaspar, H. B. Familial haemophagocytic lymphohistiocytosis: advances in the genetic basis, diagnosis and management. *Clin. Exp. Immunol.* **2011**, *163* (3), 271–83.
(62) How, P. C.; Shields, D. Tethering function of the caspase cleavage fragment of Golgi protein p115 promotes apoptosis via a p53-dependent pathway. *J. Biol. Chem.* **2011**, *286* (10), 8565–76.
(63) Radulescu, A. E.; Mukherjee, S.; Shields, D. The Golgi protein p115 associates with gamma-tubulin and plays a role in Golgi structure and mitosis progression. *J. Biol. Chem.* **2011**, *286* (24), 21915–26.
(64) Bouffard, P.; Hayashi, P. H.; Acevedo, R.; Levy, N.; Zeldis, J. B. Hepatitis C virus is detected in a monocyte/macrophage subpopulation of peripheral blood mononuclear cells of infected patients. *J. Infect. Dis.* **1992**, *166* (6), 1276–80.
(65) Roxrud, I.; Raiborg, C.; Pedersen, N. M.; Stang, E.; Stenmark, H. An endosomally localized isoform of Eps15 interacts with Hrs to mediate degradation of epidermal growth factor receptor. *J. Cell Biol.* **2008**, *180* (6), 1205–18.
(66) Salcini, A. E.; Chen, H.; Iannolo, G.; De Camilli, P.; Di Fiore, P. P. Epidermal growth factor pathway substrate 15, Eps15. *Int. J. Biochem. Cell Biol.* **1999**, *31* (8), 805–9.
(67) Barnaba, V. Hepatitis C virus infection: a "liaison a trois" amongst the virus, the host, and chronic low-level inflammation for human survival. *J. Hepatol.* **2010**, *53* (4), 752–61.
(68) Hiroishi, K.; Ito, T.; Imawari, M. Immune responses in hepatitis C virus infection and mechanisms of hepatitis C virus persistence. *J. Gastroenterol. Hepatol.* **2008**, *23* (10), 1473–82.
(69) Kawai, T.; Akira, S. Toll-like receptor and RIG-I-like receptor signaling. *Ann. N.Y. Acad. Sci.* **2008**, *1143*, 1–20.
(70) Sklan, E. H.; Charuworn, P.; Pang, P. S.; Glenn, J. S. Mechanisms of HCV survival in the host. *Nat. Rev. Gastroenterol. Hepatol.* **2009**, *6* (4), 217–27.
(71) Szabo, G.; Dolganiuc, A. Hepatitis C and innate immunity: recent advances. *Clin. Liver Dis.* **2008**, *12* (3), 675–92.
(72) Taylor, D. R.; Silberstein, E. Innate immunity and hepatitis C virus: eluding the host cell defense. *Front. Biosci.* **2009**, *14*, 4950–61.
(73) Legarda-Addison, D.; Hase, H.; O'Donnell, M. A.; Ting, A. T. NEMO/IKKgamma regulates an early NF-kappaB-independent cell-death checkpoint during TNF signaling. *Cell Death Differ.* **2009**, *16* (9), 1279–88.
(74) Ye, X.; Lu, H.; Huo, K.; Chen, D. Finding a novel interacting protein of the hepatic carcinoma related gene MIP: NF-kappaB essential modulator (NEMO). *Oncol. Rep.* **2011**, *25* (1), 231–5.
(75) Beraza, N.; Malato, Y.; Sander, L. E.; Al-Masaoudi, M.; Freimuth, J.; Riethmacher, D.; Gores, G. J.; Roskams, T.; Liedtke, C.; Trautwein, C. Hepatocyte-specific NEMO deletion promotes NK/NKT cell- and TRAIL-dependent liver damage. *J. Exp. Med.* **2009**, *206* (8), 1727–37.
(76) Cruz-Munoz, M. E.; Veillette, A. Do NK cells always need a license to kill? *Nat. Immunol.* **2010**, *11* (4), 279–80.
(77) Wang, K.; Song, Y.; Chen, D. B.; Zheng, J. Protein phosphatase 3 differentially modulates vascular endothelial growth factor- and fibroblast growth factor 2-stimulated cell proliferation and signaling in ovine fetoplacental artery endothelial cells. *Biol. Reprod.* **2008**, *79* (4), 704–10.
(78) Singh, A. P.; Bafna, S.; Chaudhary, K.; Venkatraman, G.; Smith, L.; Eudy, J. D.; Johansson, S. L.; Lin, M. F.; Batra, S. K. Genome-wide expression profiling reveals transcriptomic variation and perturbed gene networks in androgen-dependent and androgen-independent prostate cancer cells. *Cancer Lett.* **2008**, *259* (1), 28–38.
(79) Ostenfeld, M. S.; Bramsen, J. B.; Lamy, P.; Villadsen, S. B.; Fristrup, N.; Sorensen, K. D.; Ulhoi, B.; Borre, M.; Kjems, J.; Dyrskjot, L.; Orntoft, T. F. miR-145 induces caspase-dependent and -independent cell death in urothelial cancer cell lines with targeting of an expression signature present in Ta bladder tumors. *Oncogene* **2010**, *29* (7), 1073–84.

(80) Johansen, C.; Vestergaard, C.; Kragballe, K.; Kollias, G.; Gaestel, M.; Iversen, L. MK2 regulates the early stages of skin tumor promotion. *Carcinogenesis* **2009**, *30* (12), 2100–8.
(81) Wang, C.; Zhou, J.; Wang, S.; Ye, M.; Fan, G.; Zou, H.; Jiang, C. Shotgun approach based comparative proteomic analysis of levo-tetrahydropalmatine-induced apoptosis in hepatocytes. *Toxicol. Lett.* **2010**, *194* (1–2), 8–15.
(82) Del Campo, J. A.; Romero-Gomez, M. Steatosis and insulin resistance in hepatitis C: a way out for the virus? *World J. Gastroenterol.* **2009**, *15* (40), 5014–9.
(83) Douglas, M. W.; George, J. Molecular mechanisms of insulin resistance in chronic hepatitis C. *World J. Gastroenterol.* **2009**, *15* (35), 4356–64.
(84) Shintani, Y.; Fujie, H.; Miyoshi, H.; Tsutsumi, T.; Tsukamoto, K.; Kimura, S.; Moriya, K.; Koike, K. Hepatitis C virus infection and diabetes: direct involvement of the virus in the development of insulin resistance. *Gastroenterology* **2004**, *126* (3), 840–8.
(85) Cao, X.; Pobezinskaya, Y. L.; Morgan, M. J.; Liu, Z. G. The role of TRADD in TRAIL-induced apoptosis and signaling. *FASEB J.* **2011**, *25* (4), 1353–8.
(86) Zheng, L.; Bidere, N.; Staudt, D.; Cubre, A.; Orenstein, J.; Chan, F. K.; Lenardo, M. Competitive control of independent programs of tumor necrosis factor receptor-induced cell death by TRADD and RIP1. *Mol. Cell. Biol.* **2006**, *26* (9), 3505–13.
(87) Tellinghuisen, T. L.; Foss, K. L.; Treadaway, J. Regulation of hepatitis C virion production via phosphorylation of the NS5A protein. *PLoS Pathog.* **2008**, *4* (3), e1000032.
(88) Benedicto, I.; Molina-Jimenez, F.; Bartosch, B.; Cosset, F. L.; Lavillette, D.; Prieto, J.; Moreno-Otero, R.; Valenzuela-Fernandez, A.; Aldabe, R.; Lopez-Cabrera, M.; Majano, P. L. The tight junction-associated protein occludin is required for a postbinding step in hepatitis C virus entry and infection. *J. Virol.* **2009**, *83* (16), 8012–20.
(89) Bantel, H.; Schulze-Osthoff, K. Apoptosis in hepatitis C virus infection. *Cell Death Differ.* **2003**, *10* (Suppl 1), S48–58.
(90) Deng, L.; Adachi, T.; Kitayama, K.; Bungyoku, Y.; Kitazawa, S.; Ishido, S.; Shoji, I.; Hotta, H. Hepatitis C virus infection induces apoptosis through a Bax-triggered, mitochondrion-mediated, caspase 3-dependent pathway. *J. Virol.* **2008**, *82* (21), 10375–85.
(91) Fischer, R.; Baumert, T.; Blum, H. E. Hepatitis C virus infection and apoptosis. *World J. Gastroenterol.* **2007**, *13* (36), 4865–72.
(92) Hanafy, S. M.; Shehata, O. H.; Farahat, N. M. Expression of apoptotic markers BCL-2 and Bax in chronic hepatitis C virus patients. *Clin. Biochem.* **2010**, *43* (13–14), 1112–7.
(93) Joyce, M. A.; Walters, K. A.; Lamb, S. E.; Yeh, M. M.; Zhu, L. F.; Kneteman, N.; Doyle, J. S.; Katze, M. G.; Tyrrell, D. L. HCV induces oxidative and ER stress, and sensitizes infected cells to apoptosis in SCID/Alb-uPA mice. *PLoS Pathog.* **2009**, *5* (2), e1000291.
(94) Kondo, Y.; Machida, K.; Liu, H. M.; Ueno, Y.; Kobayashi, K.; Wakita, T.; Shimosegawa, T.; Lai, M. M. Hepatitis C virus infection of T cells inhibits proliferation and enhances fas-mediated apoptosis by down-regulating the expression of CD44 splicing variant 6. *J. Infect. Dis.* **2009**, *199* (5), 726–36.
(95) Anupam, R.; Datta, A.; Kesic, M.; Green-Church, K.; Shkriabai, N.; Kvaratskhelia, M.; Lairmore, M. D. Human T-lymphotropic virus type 1 p30 interacts with REGgamma and modulates ATM (ataxia telangiectasia mutated) to promote cell survival. *J. Biol. Chem.* **2011**, *286* (9), 7661–8.
(96) Mao, I.; Liu, J.; Li, X.; Luo, H. REGgamma, a proteasome activator and beyond? *Cell. Mol. Life Sci.* **2008**, *65* (24), 3971–80.
(97) Tian, M.; Xiaoyi, W.; Xiaotao, L.; Guosheng, R. Proteasomes reactivator REG gamma enchances oncogenicity of MDA-MB-231 cell line via promoting cell proliferation and inhibiting apoptosis. *Cell. Mol. Biol. (Noisy-le-Grand)* **2009**, *55* (Suppl), OL1121–31.
(98) Zannini, L.; Buscemi, G.; Fontanella, E.; Lisanti, S.; Delia, D. REGgamma/PA28gamma proteasome activator interacts with PML and Chk2 and affects PML nuclear bodies number. *Cell Cycle* **2009**, *8* (15), 2399–407.
(99) Samuelsen, J. T.; Schwarze, P. E.; Huitfeldt, H. S.; Thrane, E. V.; Lag, M.; Refsnes, M.; Skarpen, E.; Becher, R. Regulation of rat alveolar type 2 cell proliferation in vitro involves type II cAMP-dependent protein kinase. *Am. J. Physiol. Lung Cell. Mol. Physiol.* **2007**, *292* (1), L232–9.
(100) Bungyoku, Y.; Shoji, I.; Makine, T.; Adachi, T.; Hayashida, K.; Nagano-Fujii, M.; Ide, Y. H.; Deng, L.; Hotta, H. Efficient production of infectious hepatitis C virus with adaptive mutations in cultured hepatoma cells. *J. Gen. Virol.* **2009**, *90* (Pt 7), 1681–91.
(101) Lemon, S. M.; McKeating, J. A.; Pietschmann, T.; Frick, D. N.; Glenn, J. S.; Tellinghuisen, T. L.; Symons, J.; Furman, P. A. Development of novel therapies for hepatitis C. *Antiviral Res.* **2010**, *86* (1), 79–92.
(102) Lin, K. Development of novel antiviral therapies for hepatitis C virus. *Virol. Sin.* **2010**, *25* (4), 246–66.
(103) Chan, S. C.; Lo, S. Y.; Liou, J. W.; Lin, M. C.; Syu, C. L.; Lai, M. J.; Chen, Y. C.; Li, H. C. Visualization of the structures of the hepatitis C virus replication complex. *Biochem. Biophys. Res. Commun.* **2011**, *404* (1), 574–8.
(104) Dreyer, J. L. Lentiviral vector-mediated gene transfer and RNA silencing technology in neuronal dysfunctions. *Mol. Biotechnol.* **2011**, *47* (2), 169–87.
(105) Camm, E. J.; Martin-Gronert, M. S.; Wright, N. L.; Hansell, J. A.; Ozanne, S. E.; Giussani, D. A. Prenatal hypoxia independent of undernutrition promotes molecular markers of insulin resistance in adult offspring. *FASEB J.* **2011**, *25* (1), 420–7.
(106) Ning, B. F.; Ding, J.; Yin, C.; Zhong, W.; Wu, K.; Zeng, X.; Yang, W.; Chen, Y. X.; Zhang, J. P.; Zhang, X.; Wang, H. Y.; Xie, W. F. Hepatocyte nuclear factor 4 alpha suppresses the development of hepatocellular carcinoma. *Cancer Res.* **2010**, *70* (19), 7640–51.
(107) Niehof, M.; Borlak, J. EPS15R, TASP1, and PRPF3 are novel disease candidate genes targeted by HNF4alpha splice variants in hepatocellular carcinomas. *Gastroenterology* **2008**, *134* (4), 1191–202.
(108) Hussain, K. M.; Leong, K. L.; Ng, M. M.; Chu, J. J. The essential role of clathrin-mediated endocytosis in the infectious entry of human enterovirus 71. *J. Biol. Chem.* **2011**, *286* (1), 309–21.
(109) Helle, F.; Dubuisson, J. Hepatitis C virus entry into host cells. *Cell. Mol. Life Sci.* **2008**, *65* (1), 100–12.
(110) Marshall, A.; Rushbrook, S.; Morris, L. S.; Scott, I. S.; Vowler, S. L.; Davies, S. E.; Coleman, N.; Alexander, G. Hepatocyte expression of minichromosome maintenance protein-2 predicts fibrosis progression after transplantation for chronic hepatitis C virus: a pilot study. *Liver Transpl.* **2005**, *11* (4), 427–33.
(111) Bard-Chapeau, E. A.; Li, S.; Ding, J.; Zhang, S. S.; Zhu, H. H.; Princen, F.; Fang, D. D.; Han, T.; Bailly-Maitre, B.; Poli, V.; Varki, N. M.; Wang, H.; Feng, G. S. Ptpn11/Shp2 acts as a tumor suppressor in hepatocellular carcinogenesis. *Cancer Cell* **2011**, *19* (5), 629–39.
(112) Matsuo, K.; Delibegovic, M.; Matsuo, I.; Nagata, N.; Liu, S.; Bettaieb, A.; Xi, Y.; Araki, K.; Yang, W.; Kahn, B. B.; Neel, B. G.; Haj, F. G. Altered glucose homeostasis in mice with liver-specific deletion of Src homology phosphatase 2. *J. Biol. Chem.* **2010**, *285* (51), 39750–8.
(113) Rios, E. J.; Piliponsky, A. M.; Ra, C.; Kalesnikoff, J.; Galli, S. J. Rabaptin-5 regulates receptor expression and functional activation in mast cells. *Blood* **2008**, *112* (10), 4148–57.
(114) Stenmark, H.; Vitale, G.; Ullrich, O.; Zerial, M. Rabaptin-5 is a direct effector of the small GTPase Rab5 in endocytic membrane fusion. *Cell* **1995**, *83* (3), 423–32.
(115) Edamoto, Y.; Hara, A.; Biernat, W.; Terracciano, L.; Cathomas, G.; Riehle, H. M.; Matsuda, M.; Fujii, H.; Scoazec, J. Y.; Ohgaki, H. Alterations of RB1, p53 and Wnt pathways in hepatocellular carcinomas associated with hepatitis C, hepatitis B and alcoholic liver cirrhosis. *Int. J. Cancer* **2003**, *106* (3), 334–41.
(116) Laurent-Puig, P.; Zucman-Rossi, J. Genetics of hepatocellular tumors. *Oncogene* **2006**, *25* (27), 3778–86.
(117) Park, K. J.; Choi, S. H.; Koh, M. S.; Kim, D. J.; Yie, S. W.; Lee, S. Y.; Hwang, S. B. Hepatitis C virus core protein potentiates c-Jun N-terminal kinase activation through a signaling complex involving TRADD and TRAF2. *Virus Res.* **2001**, *74* (1–2), 89–98.
(118) Kawaguchi, T.; Yoshida, T.; Harada, M.; Hisamoto, T.; Nagao, Y.; Ide, T.; Taniguchi, E.; Kumemura, H.; Hanada, S.; Maeyama, M.;

Baba, S.; Koga, H.; Kumashiro, R.; Ueno, T.; Ogata, H.; Yoshimura, A.; Sata, M. Hepatitis C virus down-regulates insulin receptor substrates 1 and 2 through up-regulation of suppressor of cytokine signaling 3. *Am. J. Pathol.* **2004**, *165* (5), 1499–508.

(119) Ma, Z.; Liu, Z.; Wu, R. F.; Terada, L. S. p66(Shc) restrains Ras hyperactivation and suppresses metastatic behavior. *Oncogene* **2010**, *29* (41), 5559–67.

(120) Spoden, G. A.; Rostek, U.; Lechner, S.; Mitterberger, M.; Mazurek, S.; Zwerschke, W. Pyruvate kinase isoenzyme M2 is a glycolytic sensor differentially regulating cell proliferation, cell size and apoptotic cell death dependent on glucose supply. *Exp. Cell Res.* **2009**, *315* (16), 2765–74.

JVI
Journals.ASM.org

# Expression of MicroRNA miR-122 Facilitates an Efficient Replication in Nonhepatic Cells upon Infection with Hepatitis C Virus

Takasuke Fukuhara,[a] Hiroto Kambara,[a] Mai Shiokawa,[a] Chikako Ono,[a] Hiroshi Katoh,[a] Eiji Morita,[a] Daisuke Okuzaki,[b] Yoshihiko Maehara,[c] Kazuhiko Koike,[d] and Yoshiharu Matsuura[a]

Department of Molecular Virology[a] and DNA-Chip Developmental Center for Infectious Diseases,[b] Research Institute for Microbial Diseases, Osaka University, Osaka, Japan; Department of Surgery and Science, Graduate School of Medical Sciences, Kyushu University, Fukuoka, Japan[c]; and Department of Gastroenterology, Graduate School of Medicine, University of Tokyo, Tokyo, Japan[d]

**Hepatitis C virus (HCV) is one of the most common etiologic agents of chronic liver diseases, including liver cirrhosis and hepatocellular carcinoma. In addition, HCV infection is often associated with extrahepatic manifestations (EHM), including mixed cryoglobulinemia and non-Hodgkin's lymphoma. However, the mechanisms of cell tropism of HCV and HCV-induced EHM remain elusive, because *in vitro* propagation of HCV has been limited in the combination of cell culture-adapted HCV (HCVcc) and several hepatic cell lines. Recently, a liver-specific microRNA called miR-122 was shown to facilitate the efficient propagation of HCVcc in several hepatic cell lines. In this study, we evaluated the importance of miR-122 on the replication of HCV in nonhepatic cells. Among the nonhepatic cell lines expressing functional HCV entry receptors, Hec1B cells derived from human uterus exhibited a low level of replication of the HCV genome upon infection with HCVcc. Exogenous expression of miR-122 in several cells facilitates efficient viral replication but not production of infectious particles, probably due to the lack of hepatocytic lipid metabolism. Furthermore, expression of mutant miR-122 carrying a substitution in a seed domain was required for efficient replication of mutant HCVcc carrying complementary substitutions in miR-122-binding sites, suggesting that specific interaction between miR-122 and HCV RNA is essential for the enhancement of viral replication. In conclusion, although miR-122 facilitates efficient viral replication in nonhepatic cells, factors other than miR-122, which are most likely specific to hepatocytes, are required for HCV assembly.**

More than 170 million individuals worldwide are infected with hepatitis C virus (HCV), and cirrhosis and hepatocellular carcinoma induced by HCV infection are life-threatening diseases (57). Although therapy combining pegylated interferon (IFN) and ribavirin has achieved a sustained virological response in 50% of individuals infected with HCV genotype 1 (37), a more effective therapeutic modality for HCV infection is needed (46). The establishment of *in vivo* and *in vitro* infection systems has been hampered by the narrow host range and tissue tropism of HCV. Although the chimpanzee is the only experimental animal susceptible to HCV infection, it is difficult to use the chimpanzee in experiments due to ethical concerns (3). Furthermore, robust *in vitro* HCV propagation is limited to the combination of cell culture-adapted clones based on the genotype 2a JFH1 strain (HCVcc) and human hepatoma cell lines, including Huh7, Hep3B, and HepG2 (29, 43, 62).

It is well-known that HCV mainly infects hepatocytes. However, the precise mechanism underlying the liver tropism of HCV has not been clarified. Chronic hepatitis C virus infection is often associated with at least one extrahepatic manifestation (EHM), including mixed cryoglobulinemia, non-Hodgkin's lymphoma, lichen planus, thyroiditis, diabetes mellitus, Sjögren syndrome, and arthritis (19). EHMs are frequently more serious than hepatic disease in some patients and sometimes occur even in patients with persistently normal liver functions (19). Mixed cryoglobulinemia is the most-well-characterized HCV-associated disease and is curable by viral clearance through antiviral therapies (6). Although replication of HCV RNA in peripheral blood mononuclear cells (PBMCs) and neuronal cells at a low level was suggested (64), the biological significance of the extrahepatic replication of HCV, particularly in the development of EHMs, is not well understood.

MicroRNAs (miRNAs) are small noncoding RNAs consisting of 20 to 25 nucleotides that modulate gene expression in plants and animals (1, 24). Most miRNAs negatively regulate translation through the interaction with the 3′ untranslated region (UTR) of mRNA in a sequence-specific manner. miRNA 122 (miR-122) is liver specific, is the most abundantly expressed miRNA in the liver, and represses the translation of several mRNAs (5, 7). Jopling et al. reported for the first time that the inhibition of miR-122 dramatically decreased RNA replication in HCV subgenomic replicon (SGR) cells (28). In addition, several reports revealed that a specific interaction between the seed domain of miR-122 and the complementary sequences in the 5′ UTR of HCV RNA is essential for the enhancement of translation and replication of the HCV genome (21, 25, 27, 36). Endogenous expression levels of miR-122 are significantly higher in Huh7 cells than in other hepatic and nonhepatic cell lines (Fig. 1). In addition, previous reports showed that miR-122 expression enhanced the replication of SGR RNA in human embryonic kidney 293 (HEK293) cells and mouse embryonic fibroblasts (MEFs) (8, 35). Furthermore, it was recently shown that exogenous expression of miR-122 facilitates the efficient propagation of HCVcc in Hep3B and HepG2 cells, which are

Received 4 March 2012 Accepted 10 May 2012
Published ahead of print 16 May 2012
Address correspondence to Yoshiharu Matsuura, matsuura@biken.osaka-u.ac.jp.

doi:10.1128/JVI.00567-12

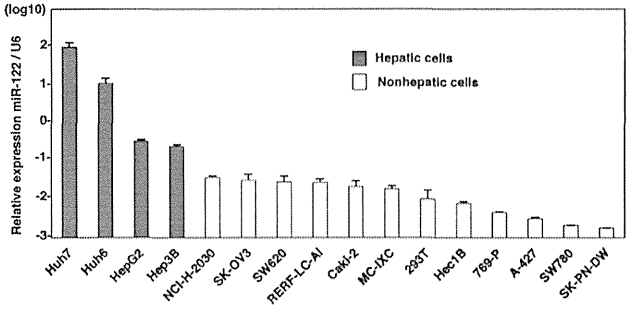


FIG 1 Endogenous expression levels of miR-122 in hepatic and nonhepatic cells. Total miRNAs were extracted from Huh7, Huh6, HepG2, Hep3B, NCI-H-2030, SK-OV3, SW620, RERF-LC-AI, Caki-2, MC-IXC, 293T, Hec1B, 769-P, A-427, SW780, and SK-PN-DW cells, and the expression levels of miR-122 were determined by qRT-PCR.

nonpermissive for HCVcc propagation (29, 43). These results suggest that the high susceptibility of Huh7 cells to the propagation of HCVcc is attributable to the high expression level of miR-122 and raise the possibility of expanding the HCV host range through the exogenous expression of miR-122 in nonhepatic cells.

In this study, we assessed the effect of miR-122 expression on the replication of HCVcc and SGR RNA in several nonhepatic cell lines. Although the exogenous expression of miR-122 in the cell lines facilitates significant RNA replication through a gene-specific interaction between miR-122 and 5′ UTR of HCV RNA, no infectivity was detected in either the cells or the culture supernatants. The current study suggests that the expression of miR-122 plays an important role in HCV cell tropism, as well as in the possible involvement of nonhepatic cells in EHM, through an incomplete propagation of HCV.

## MATERIALS AND METHODS

**NextBio Body Atlas.** The NextBio Body Atlas application presents an aggregated analysis of gene expression across various normal tissues, normal cell types, and cancer cell lines. It enables us to investigate the expression of individual genes as well as gene sets. Samples for Body Atlas data are obtained from publicly available studies that are internally curated, annotated, and processed (31). Body Atlas measurements are generated from all available RNA expression studies that used Affymetrix U133 Plus or U133A Genechip arrays for human studies. The results corresponding to 128 human tissue samples were incorporated from 1,067 arrays, the results corresponding to 157 human cell types were incorporated from 1,474 arrays, and the results corresponding to 359 human cancer cell lines were incorporated from 376 arrays. Gene queries return a list of relevant tissues or cell types rank ordered by absolute gene expression and grouped by body systems or across all body systems. In the current analysis, we screened for nonhepatic cell lines expressing HCV receptor candidates, including CD81, SR-BI, claudin1 (CLDN1), and occludin (OCLN), or very-low-density lipoprotein (VLDL)-associated proteins, including apolipoprotein E (ApoE), ApoB, and microsomal triglyceride transfer protein (MTTP). A detailed analysis protocol developed by NextBio was described previously (31). The raw data used in this application are derived from the GSK Cancer Cell Line data deposited at the National Cancer Institute website (https://array.nci.nih.gov/caarray/project/woost-00041) and additionally from NCBI Gene Expression Omnibus (GEO) accession number GSE5720 for cell lines SK-OV-3 and SW620.

**Sample collection and RNA extraction for microarray analysis.** Total RNAs extracted from cells were purified by using an miRNeasy kit (Qiagen, Valencia, CA) according to the manufacturer's protocol. Eluted RNAs were quantified using a Nanodrop ND-1000 (version 3.5.2) spectrophotometer (Thermo Scientific, Wartham, MA). RNA integrity was evaluated using the RNA 6000 LabChip kit and bioanalyzer (Agilent Technologies, Santa Clara, CA). Each RNA that had an RNA integrity number (RIN) greater than 9.0 was used for the microarray experiments.

**Microarray experiment.** Expression profiling was generated using the 4 × 44K whole-human-genome oligonucleotide microarray (version 2.0) G4845A (Agilent Technologies). Each microarray uses 44,495 probes to interrogate 27,958 Entrez gene RNAs. One hundred nanograms of total RNA was reverse transcribed into double-stranded cDNAs by AffinityScript multiple-temperature reverse transcriptase and amplified for 2 h at 40°C. The resulting cDNAs were subsequently used for *in vitro* transcription by the T7 polymerase and labeled with cyanine-3-labeled cytosine triphosphate (Perkin Elmer, Waltham, MA) for 2 h at 40°C using a low-input Quick-Amp labeling kit (Agilent Technologies) according to the manufacturer's protocol. After labeling, the rates of dye incorporation and quantification were measured with a Nanodrop ND-1000 (version 3.5.2) spectrophotometer (Thermo Scientific), and then the cRNAs were fragmented for 30 min at 60°C in the dark. Differentially labeled samples of 1,650 ng of cRNA were hybridized on Agilent 4 × 44K whole-genome arrays (version 2.0; 026652; Agilent Design) at 65°C for 17 h with rotation in the dark. Hybridization was performed using a gene expression hybridization kit (Agilent Technologies) following the manufacturer's instructions. After washing in gene expression washing buffer, each slide was scanned with the Agilent microarray scanner G2505C. Feature extraction software (version 10.5.1.1) employing defaults for all parameters was used to convert the images into gene expression data. Raw data were imported into a Subio platform (version 1.12) for database management and quality control. Raw intensity data were normalized against GAPDH (glyceraldehyde-3-phosphate dehydrogenase) expression levels for further analysis. These raw data have been accepted by GEO (a public repository for microarray data aimed at storing minimum information about microarray experiments [MIAME]).

**Plasmids.** The cDNA clones of wild-type (WT) and mutant (MT) pri-miR-122 and *Aequorea coerulescens* green fluorescent protein (AcGFP) were inserted between the XhoI and XbaI sites of lentiviral vector pCSII-EF-RfA, which was kindly provided by M. Hijikata, and the resulting plasmids were designated pCSII-EF-WT-miR-122, pCSII-EF-MT-miR-122, and pCSII-EF-AcGFP, respectively. Plasmids pHH-JFH1 and pSGR-JFH1, which encode full-length and subgenomic cDNA of the JFH1 strain, respectively, were kindly provided by T. Wakita. pHH-JFH1-E2p7NS2mt contains three adaptive mutations in pHH-JFH1 (53). pHH-JFH1-M1 and pHH-JFH1-M2 were established by the introduction of a point mutation of nucleotide 26 located in site 1 and nucleotide 41 in site 2 of the 5′ UTR of the JFH1 cDNA construct pHH-JFH1. pSGR-Con1, which encodes SGR of the Con1 strain, was kindly provided by R. Bartenschlager. The complementary sequences of miR-122 were introduced into the multicloning site of the pmirGLO vector (Promega, Madison, WI), and the resulting plasmid was designated pmirGLO-compl-miR-122. The plasmids used in this study were confirmed by sequencing with an ABI 3130 genetic analyzer (Applied Biosystems, Tokyo, Japan).

**Cell lines.** All cell lines were cultured at 37°C under the conditions of a humidified atmosphere and 5% $CO_2$. The following cells were maintained in Dulbecco modified Eagle medium (DMEM; Sigma-Aldrich, St. Louis, MO) supplemented with 100 U/ml penicillin, 100 μg/ml streptomycin, and 10% fetal calf serum (FCS): human hepatocellular carcinoma-derived Huh7, Hep3B, and HepG2; embryonic kidney-derived HEK293 and 293T; lung-derived RERF-LC-AI, NCI-H-2030, and A-427; kidney-derived Caki-2 and 769-P; neuron-derived MC-IXC and SK-PN-DW; uterus-derived Hec1B; ovary-derived SK-OV3; colon-derived SW620; and urinary bladder-derived SW780 cells. RERF-LC-AI (RCB0444) cells were provided by the RIKEN BRC through the National Bio-Resource Project of MEXT, Japan. Hec1B (JCRB1193) cells were obtained from the JCRB Cell Bank. NCI-H-2030, A-427, Caki-2, 769-P, MC-IXC, SK-PN-DW, SK-OV3, and SW780 cells were obtained from the American Type Culture Collection (ATCC). SW620 cells were kindly provided by C.

Oneyama. 293T-CLDN cells stably expressing CLDN1 were established by the introduction of the expression plasmids encoding CLDN1 under the control of the CAG promoter of pCAG-pm3. The Huh7-derived cell line Huh7.5.1 was kindly provided by F. Chisari. The Huh7OK1 cell line efficiently propagates HCVcc as previously described (45). Huh7, Hec1B, and HEK293 cells harboring Con1- or JFH1-based HCV SGR were prepared according to the method described in a previous report (47) and maintained in DMEM containing 10% FCS and 1 mg/ml G418 (Nakalai Tesque, Kyoto, Japan).

**Antibodies and drugs.** Mouse monoclonal antibodies to HCV nonstructural protein 5A (NS5A) and β-actin were purchased from Austral Biologicals (San Ramon, CA) and Sigma-Aldrich, respectively. Mouse anti-ApoE antibody was purchased from Santa Cruz Biotechnology (Santa Cruz, CA). Rabbit anti-HCV core protein and NS5A were prepared as described previously (41). Rabbit anti-SR-BI antibody was purchased from Novus Biologicals (Littleton, CO). Rabbit anti-CLDN1 and -OCLN antibodies, Alexa Fluor 488 (AF488)-conjugated anti-rabbit or -mouse IgG antibodies, and AF594-conjugated anti-mouse IgG2a antibodies were purchased from Invitrogen (San Diego, CA). Mouse anti-FKBP8 antibody was described previously (44). Mouse anti-double-stranded RNA (anti-dsRNA) IgG2a (J1 and K2) antibodies were obtained from Biocenter Ltd. (Szirak, Hungary). The HCV NS3/4A protease inhibitor was purchased from Acme Bioscience (Salt Lake City, UT). Human recombinant alpha IFN (IFN-α) and cyclosporine were purchased from PBL Biomedical Laboratories (Piscataway, NJ) and Sigma-Aldrich, respectively. BODIPY 558/568 lipid probe was purchased from Invitrogen. The locked nucleic acid (LNA) targeted to miR-122, LNA-miR-122 (5′-CcAttGTcaCaCtCC-3′), and its negative control, LNA-control (5′-CcAttCTgaCcCtAC-3′) (LNAs are in capital letters, DNAs are in lowercase letters; sulfur atoms in oligonucleotide phosphorothioates are substituted for nonbridging oxygen atoms; the capital C indicates LNA methylcytosine), were purchased from Gene Design (Osaka, Japan) (15).

**Preparation of viruses.** pHH-JFH1-E2p7NS2mt was introduced into Huh7.5.1 cells, HCVcc in the supernatant was collected after serial passages (39), and infectious titers were determined by a focus-forming assay and expressed in focus-forming units (FFUs) (62). Mutant HCVcc was produced from Huh7.5.1 cells expressing MT miR-122 according to the method of a previous report with minor modifications (25). HCVpv, a pseudotype vesicular stomatitis virus (VSV) bearing HCV E1 and E2 glycoproteins, was prepared as previously described (61), and infectivity was assessed by luciferase expression on a Bright-Glo luciferase assay system (Promega), following a protocol provided by the manufacturer and expressed in relative light units (RLUs).

**Lipofection and lentiviral gene transduction.** Cells were transfected with the plasmids by using Trans IT LT-1 transfection reagent (Mirus, Madison, WI) according to the manufacturer's protocol. LNAs were introduced into cells by Lipofectamine RNAiMAX (Invitrogen). The lentiviral vectors and ViraPower lentiviral packaging mix (Invitrogen) were cotransfected into 293T cells, and the supernatants were recovered at 48 h posttransfection. The lentivirus titer was determined by a Lenti-XTM quantitative reverse transcription-PCR (qRT-PCR) titration kit (Clontech, Mountain View, CA), and the expression levels of miR-122 and AcGFP were determined at 48 h postinoculation.

**Quantitative RT-PCR.** HCV RNA levels were determined by the method described previously (18). Total RNA was extracted from cells by using an RNeasy minikit (Qiagen). The first-strand cDNA synthesis and qRT-PCR were performed with TaqMan EZ RT-PCR core reagents and an ABI Prism 7000 system (Applied Biosystems), respectively, according to the manufacturer's protocols. The primers for TaqMan PCR targeted to the noncoding region of HCV RNA were synthesized as previously reported (42). To determine the expression levels of miR-122, total miRNA was prepared by using the miRNeasy minikit, and miR-122 expression was determined by using fully processed miR-122-specific RT and PCR primers provided in the TaqMan microRNA assays according to the manufacturer's protocol. U6 small nuclear RNA was used as an internal control. Fluorescent signals were analyzed with the ABI Prism 7000 system.

**Immunoblotting.** Cells were lysed on ice in lysis buffer (20 mM Tris-HCl [pH 7.4], 135 mM NaCl, 1% Triton X-100, 10% glycerol) supplemented with a protease inhibitor mix (Nacalai Tesque). The samples were boiled in loading buffer and subjected to 5 to 20% gradient SDS-PAGE. The proteins were transferred to polyvinylidene difluoride membranes (Millipore, Bedford, MA) and reacted with the appropriate antibodies. The immune complexes were visualized with SuperSignal West Femto substrate (Pierce, Rockford, IL) and detected with an LAS-3000 image analyzer system (Fujifilm, Tokyo, Japan).

**Immunofluorescence assay.** Cells cultured on glass slides were fixed with 4% paraformaldehyde (PFA) in phosphate-buffered saline (PBS) at room temperature for 30 min, permeabilized for 20 min at room temperature with PBS containing 0.2% Triton, after being washed three times with PBS, and blocked with PBS containing 2% FCS for 1 h at room temperature. The cells were incubated with PBS containing appropriate primary antibodies at room temperature for 1 h, washed three times with PBS, and incubated with PBS containing AF488- or AF594-conjugated secondary antibodies at room temperature for 1 h. For lipid droplet staining, cells incubated in medium containing 20 μg/ml BODIPY for 20 min at 37°C were washed with prewarmed fresh medium and incubated for 20 min at 37°C. Cell nuclei were stained with DAPI (4′,6-diamidino-2-phenylindole). Cells were observed with a FluoView FV1000 laser scanning confocal microscope (Olympus, Tokyo, Japan).

***In vitro* transcription, RNA transfection, and colony formation.** The plasmids pSGR-Con1 and pSGR-JFH1 were linearized with ScaI and XbaI, respectively, and treated with mung bean exonuclease. The linearized DNA was transcribed *in vitro* by using a MEGAscript T7 kit (Applied Biosystems) according to the manufacturer's protocol. The *in vitro*-transcribed RNA (10 μg) was electroporated into Hec1B and HEK293 cells at $10^7$ cells/0.4 ml under conditions of 190 V and 975 μF using a Gene Pulser apparatus (Bio-Rad, Hercules, CA) and plated on DMEM containing 10% FCS. The medium was replaced with fresh DMEM containing 10% FCS and 1 mg/ml G418 at 24 h posttransfection. The remaining colonies were cloned by using a cloning ring (Asahi Glass, Tokyo, Japan) or fixed with 4% PFA and stained with crystal violet at 4 weeks postelectroporation.

**Electron microscopy and correlative FM-EM analysis.** Cells were cultured on a Cell Desk polystyrene coverslip (Sumitomo Bakelite) and were fixed with 2% formaldehyde and 2.5% glutaraldehyde in 0.1 M cacodylate buffer (pH 7.4) containing 7% sucrose. Cells were postfixed for 1 h with 1% osmium tetroxide and 0.5% potassium ferrocyanide in 0.1 M cacodylate buffer (pH 7.4), dehydrated in graded series of ethanol, and embedded in Epon812 (TAAB). Ultrathin (80-nm) sections were stained with saturated uranyl acetate and lead citrate solution. Electron micrographs were obtained with a JEM-1011 transmission electron microscope (JEOL). Correlative fluorescence microscopy (FM)-electron microscopy (EM) allows individual cells to be examined both in an overview with FM and in a detailed subcellular-structure view with EM (51). The NS5A was stained and observed in the Hec1B-derived Con1 SGR cells by the correlative FM-EM method as described previously (44).

**Intracellular infectivity.** Intracellular viral titers were determined according to a method previously reported (20). Briefly, cells were extensively washed with PBS, scraped, and centrifuged for 5 min at 1,000 × *g*. Cell pellets were resuspended in 500 μl of DMEM containing 10% FCS and subjected to three cycles of freezing and thawing using liquid nitrogen and a thermo block set to 37°C. Cell lysates were centrifuged at 10,000 × *g* for 10 min at 4°C to remove cell debris. Cell-associated infectivity was determined by a focus-forming assay.

**Statistical analysis.** The data for statistical analyses are averages of three independent experiments. Results were expressed as means ± standard deviations. The significance of differences in the means was determined by Student's *t* test.

**Microarray data accession number.** Access to data concerning this study may be found under GEO experiment accession number GSE32886.

## RESULTS

**Nonhepatic cell lines susceptible to HCVcc by expression of miR-122.** Human CD81 (hCD81), SR-B1, CLDN1, and OCLN are crucial for HCV entry (16, 48, 49, 56). First, we examined the expression of these receptor candidates in nonhepatic cell lines by using the web-based NextBio search engine (Cupertino, CA). Multidimensional scaling was used to visualize the differences in expression patterns of molecules of various tissues, cells, and cell lines from those of hepatic cell lines and primary hepatocytes. We selected nine nonhepatic cell lines as possibly being susceptible to HCVcc infection: NCI-H-2030 (lung), Caki-2 (kidney), 769-P (bladder), A-427 (lung), SK-OV3 (ovary), SW780 (bladder), SW620 (colon), RERF-LC-AI (lung), and Hec1B (uterus) (Fig. 2). In addition, three nonhepatic cell lines previously reported to be susceptible to replication of HCV RNA—that is, SK-PN-DW (neuron), MC-IXC (neuron), and 293T-CLDN (kidney)—were included in this study (8, 17). The expression of each receptor molecule in these 12 nonhepatic cell lines was confirmed by fluorescence-activated cell sorter (FACS) analysis and immunoblotting (Fig. 3A and B). To examine the expression of the functional receptors for HCV entry in these cell lines, we inoculated HCVpv into the cells. Ten of the cell lines (A-427 and SW780 being the exceptions) exhibited various degrees of susceptibility to HCVpv infection (Fig. 3C). Therefore, we examined the possibility of propagation of HCVcc by the expression of miR-122 in these 10 cell lines.

To introduce miR-122 in the cell lines, we employed a lentiviral vector encoding pri-miR-122, an unprocessed miR-122. To confirm the maturation of pri-miR-122 to form functional RNA-induced silencing complexes (RISCs), suppression of the translation of the target mRNA was determined by a dual reporter assay. Translation of a firefly luciferase mRNA containing the sequences complementary to miR-122 in the 3′ UTR was suppressed by infection with the lentivirus encoding pri-miR-122 but not by infection with a control virus (data not shown), suggesting that the pri-miR-122 is processed into a functionally mature miR-122. By using this lentiviral vector, high levels of miR-122 expression were achieved in the 10 cell lines, comparable to the endogenous expression level of miR-122 in Huh7 cells (Fig. 4A).

To examine the effect of the exogenous expression of miR-122 on HCV replication, the nonhepatic cell lines expressing miR-122 were infected with HCVcc at a multiplicity of infection (MOI) of 1, and intracellular viral RNA was determined (Fig. 4B). The expression of miR-122 significantly increased the amount of the HCV genome in Hec1B, 293T-CLDN, MC-IXC, and RERF-LC-AI cells as well as Huh7 cells and slightly increased it in SK-OV3 and NCI-H-2030 cells. Although the levels of viral RNA in SW620, Caki-2, and SK-PN-DW cells upon expression of miR-122 were higher than those in control cells, no increase of viral RNA was observed. No effect of the expression of miR-122 was observed in 769-P cells. Interestingly, naïve Hec1B cells exhibited a delayed increase in viral RNA from 24 to 48 h postinfection, in contrast to the gradual decrease of viral RNA in other cell lines. Replication of HCV RNA in both naïve and miR-122-expressing Hec1B cells was inhibited by treatment with an inhibitor for HCV protease but not by treatment with IFN-α, due to the lack of an IFN receptor (11), whereas treatments with either IFN-α or the protease inhibitor suppressed the replication of HCV in the other cell lines expressing miR-122 (Fig. 4C). These results indicate that exogenous miR-122 expression enhances the replication of HCV even in nonhepatic cells. Hec1B cells exhibit a delayed replication of HCV, and HCV replication was enhanced by the exogenous expression of miR-122. Therefore, in this study we used Hec1B cells to investigate the biological significance of miR-122 on the replication of HCVcc in nonhepatic cells.

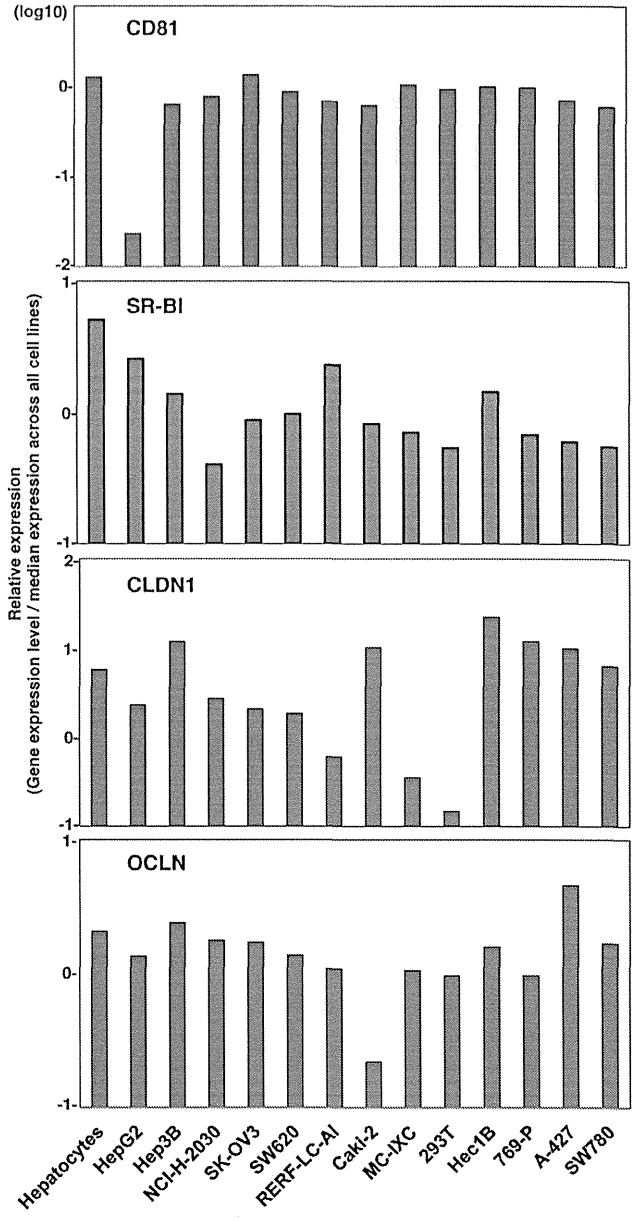


FIG 2 Receptor expression profiling in nonhepatic cells. Relative expression levels of CD81, SR-BI, CLDN1, and OCLN in primary hepatocytes, hepatic cell lines HepG2 and Hep3B, and nonhepatic cells were determined by using the NextBio Body Atlas. Expression levels were standardized by the median expression across all cell lines.

**Expression of miR-122 is essential for enhancing HCV replication in Hec1B cells.** To confirm the specificity of HCV replication in Hec1B cells, HCVcc was preincubated with an anti-HCV E2 monoclonal antibody, AP-33, or Hec1B/miR-122 and Hec1B/

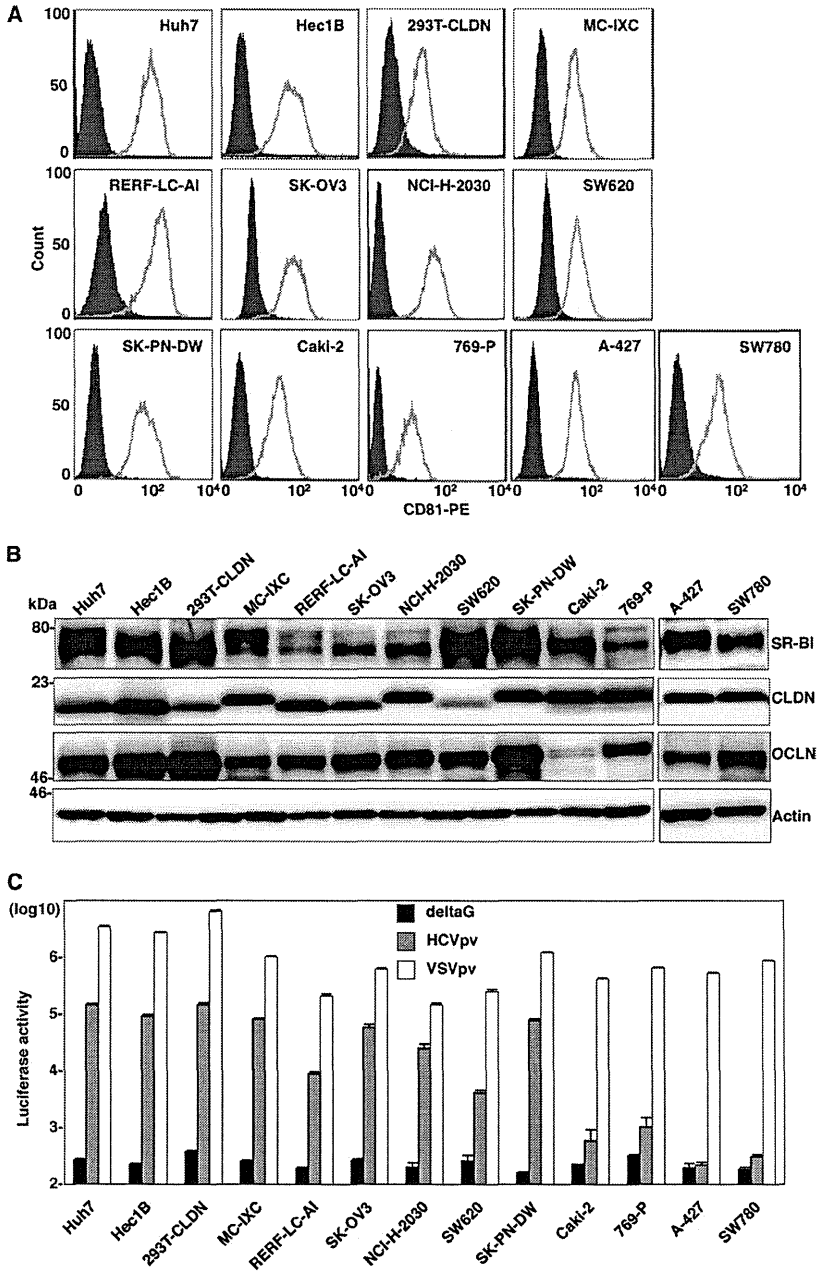


FIG 3 Expression of functional HCV receptor candidates in nonhepatic cells. (A) Expression of hCD81 in nonhepatic cells was determined by flow cytometry. PE, phycoerythrin. (B) Expression levels of SR-B1, CLDN, and OCLN in the nonhepatic cells were determined by immunoblotting. (C) The nonhepatic cell lines were inoculated with pseudotype VSVs bearing no envelope protein (deltaG), HCV envelope proteins of genotype 1b Con1 strain (HCVpv), or VSV G protein (VSVpv), and luciferase expression was determined at 24 h postinfection.

Cont cells were pretreated with anti-hCD81 monoclonal antibody. Replication of HCV RNA was determined upon infection with HCVcc. The antibody treatment significantly inhibited HCV replication in the Hec1B cell line, indicating that HCVcc internalizes into Hec1B cells through a specific interaction between hCD81 and E2 (Fig. 5). Next, we determined the dose dependence of miR-122 expression on the enhancement of HCV replication in Hec1B cells. Huh7.5.1 and Hec1B cells transduced with the lentiviral vector encoding pri-miR-122 were infected with HCVcc at an MOI of 1, and intracellular miR-122 and viral RNA were determined. Expression of miR-122 was increased in Hec1B cells in a dose-dependent manner of the lentivirus, whereas no increase was observed in Huh7.5.1 cells, probably due to the high level of endogenous expression of miR-122 (Fig. 6A, left). HCV RNA replication in Huh7.5.1 and Hec1B cells was correlated with miR-122 expression (Fig. 6A, right), suggesting a close correlation between miR-122 expression and HCV replication.

Next, we examined the expression of viral proteins in Hec1B/

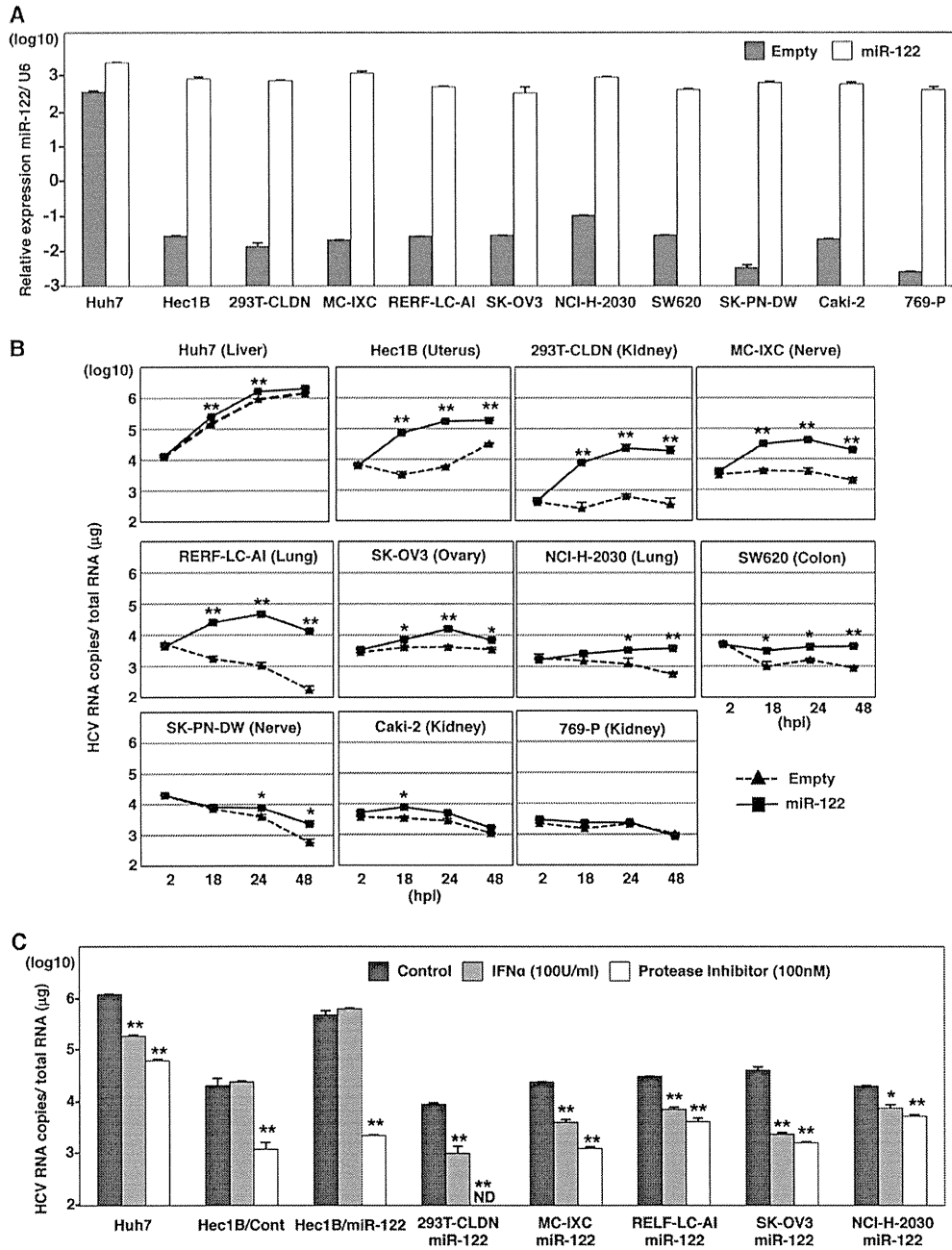


FIG 4 Nonhepatic cell lines susceptible to HCVcc by the expression of miR-122. (A) Exogenous miR-122 was expressed in Huh7, Hec1B, 293T-CLDN, MC-IXC, RERF-LC-AI, SK-OV3, NCI-H-2030, SW620, Caki-2, SK-PN-DW, and 769-P cells by lentiviral vector. Total RNA was extracted from the cells and subjected to qRT-PCR analysis. U6 was used as an internal control. Gray and white bars, endogenous and exogenous levels of miR-122, respectively. (B) HCVcc was inoculated into Huh7 and nonhepatic cell lines expressing (solid lines) or not expressing (dashed lines) exogenous miR-122 at an MOI of 1. Intracellular HCV RNA levels were determined by qRT-PCR at 2, 18, 24, and 48 h postinfection (hpi). (C) Cells were inoculated with HCVcc and simultaneously treated with either 100 U IFN-α or 100 nM HCV protease inhibitor or not treated (control), and intracellular HCV RNA levels were determined by qRT-PCR at 36 h postinfection. Asterisks indicate significant differences (*, $P < 0.05$; **, $P < 0.01$) versus the results for control cells.

miR-122 cells upon infection with HCVcc by immunoblotting and fluorescence microscopic analyses (Fig. 6B). Expression of NS5A protein was increased in Hec1B/miR-122 cells in an MOI-dependent manner. Expression of NS5A in Hec1B/Cont cells infected with HCVcc at an MOI of 3 was significantly lower than that in Hec1B/miR-122 cells infected with HCVcc at an MOI of 0.5. HCV core and NS proteins were shown to localize mainly on the lipid droplets and cytoplasmic face of the endoplasmic reticulum (ER) in Huh7 and Hep3B/miR-122 cells infected with HCVcc (29, 40). Immunofluorescence analyses revealed that HCV core and NS5A proteins were colocalized with lipid droplets and calnexin, an ER marker, in Hec1B cells infected with HCVcc (Fig. 7).

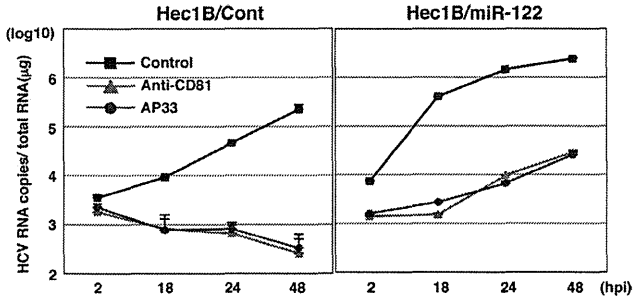


FIG 5 Neutralization of HCVcc infection in Hec1B cells by specific antibodies. HCVcc was preincubated with anti-E2 antibody (AP-33) and inoculated into Hec1B/Cont and Hec1B-miR-122 cells. Cells were preincubated with anti-human CD81 antibody and inoculated with HCVcc. Intracellular HCV RNA levels at 2, 18, 24, and 48 h postinfection were determined by qRT-PCR.

To further confirm the specificity of the enhancement of HCV replication by the expression of miR-122, Huh7, Hec1B/miR-122, and Hec1B/Cont cells were treated with LNAs that were either specific to miR-122 (LNA-miR-122) or nonspecific (LNA-control) at 6 h before infection with HCVcc. Although the treatment with LNA-miR-122 inhibited the enhancement of viral RNA replication in Huh7 and Hec1B/miR-122 cells in a dose-dependent manner, no inhibition of viral replication was observed in Hec1B/Cont cells (Fig. 6C). These results suggest that Hec1B cells permit HCV replication in a miR-122-independent manner and exogenous expression of miR-122 enhances viral replication.

**Specific interaction between miR-122 and the 5′ UTR of HCV is required for HCV replication.** To determine the effect of the specific interaction between miR-122 and the 5′ UTR of the HCV genome on the enhancement of RNA replication, we generated MT pri-miR-122 carrying a substitution of uridine to adenosine in the seed domain and an additional complementary substitution of adenosine to uridine to stabilize the loop structure of pri-miR-122 (Fig. 8A). A high expression level of MT miR-122, comparable to that of WT miR-122, was introduced into Hec1B cells by infection with lentiviral vectors (Fig. 8B). To determine the specificity of miR-122 on the replication of HCV, Hec1B cells expressing either WT or MT miR-122 were inoculated with HCVcc at an MOI of 1. Enhancement of HCV replication was observed in Hec1B cells by the expression of WT but not that of MT miR-122, suggesting that the sequence specificity of miR-122 with the 5′ UTR of HCV is crucial for the efficient replication of HCV (Fig. 8C). To further confirm the effect of the specificity of interaction between miR-122 and the binding sites in the 5′ UTR of HCV on the enhancement of HCV replication, we generated two mutant viruses, HCVcc-M1 and HCVcc-M2, carrying complementary substitutions in the miR-122-binding site 1 alone and in both sites 1 and 2 in the 5′ UTR of HCV, respectively (Fig. 8D). Recently, Jangra et al. demonstrated that the propagation of a mutant HCVcc bearing mutations in sites 1 and 2 in the 5′ UTR was rescued by the expression of MT miR-122 in Huh7.5 cells (25). We confirmed that the propagation of HCVcc-M1 and HCVcc-M2 in Huh7.5.1 cells was rescued by the expression of MT miR-122 but not of WT miR-122, although the recovery of infectious titers of HCVcc-M2 was significantly lower than the recovery of infectious titers of HCVcc-M1 (Fig. 8E). Next, to examine the interaction between miR-122 and the HCV genome in Hec1B cells, we inoculated HCVcc or mutant viruses into Hec1B cells expressing either or both WT and MT miR-122 and determined the replication of HCV RNA by qRT-PCR (Fig. 8F). Expression of WT and MT miR-122 in Hec1B cells permits replication of HCVcc and HCVcc-M2, respectively, although the enhancing effects differed. On the other hand, the expression of both WT and MT miR-122 is required for the replication of HCVcc-M1, because MT and WT miR-122 bind to sites 1 and 2 in the 5′ UTR of this virus, respectively. Interestingly, a low level of HCVcc-M1 replication was also observed in Hec1B cells expressing either WT or MT miR-122, in contrast to the requirement of the corresponding miR-122 for the replication of HCVcc and HCVcc-M2. These results suggest that the specific interaction between miR-122 and the 5′ UTR of HCV is crucial for the replication of HCV.

**Viral particle formation in hepatic and nonhepatic cells.** These data suggest that miR-122 expression facilitates replication of HCV RNA in nonhepatic cells. Recently, we have shown that expression of miR-122 facilitates infectious particle formation of HCVcc in a hepatoma cell line, Hep3B (29). To examine the effect of miR-122 expression on particle formation in nonhepatic cells, intracellular and extracellular viral RNA levels in cells infected with HCVcc were determined. Intracellular RNA replication in the hepatic cell lines, including Huh7.5.1 and Hep3B/miR-122, was increased up to 72 h postinfection with HCVcc, whereas in nonhepatic cell lines, including 293T-CLDN/miR-122 and Hec1B/miR-122, such replication was comparable to that in the hepatic cell lines until 24 h postinfection but reached a limit at this point (Fig. 9A). In spite of no clear increase of intracellular HCV RNA in Hep3B/Cont cells upon infection with HCVcc (Fig. 9A), subtle but substantial production of infectious particles was detected in the culture supernatants at 72 h postinfection, in contrast to no production of infectious particles in those of the nonhepatic cell lines (Fig. 9B). Furthermore, no focus formation was observed in Hec1B/miR-122 cells upon infection with HCVcc, in contrast to the many foci in Huh7.5.1 cells (Fig. 9C), and no infectivity was detected even in the lysates of Hec1B/miR-122 cells infected with HCVcc (Fig. 9D). These results suggest that not only the replication efficiency of viral RNA but also other factors are involved in the assembly of HCV and that the viral assembly process is impaired in Hec1B/miR-122 cells infected with HCVcc, in spite of the efficient replication of HCV RNA.

It was previously shown that lipid droplets, diacylglycerol *O*-acyltransferase 1 (DGAT1), and apolipoproteins B and E play an important role in the assembly of HCV particles (10, 22, 40). To understand the molecular mechanisms underlying the low efficiency of infectious particle formation in nonhepatic cells, we first examined the subcellular localization of lipid droplets and HCV core protein in Hec1B/miR-122 cells infected with HCVcc. Although the core protein was detected around the lipid droplets, as seen in Huh7.5.1 cells, only a small amount of lipid droplets was detected in Hec1B/miR-122 cells infected with HCVcc compared with the amount detected in Huh7.5.1 cells (Fig. 9E), suggesting that the low level of lipid droplet formation is involved in the impairment of infectious particle formation in nonhepatic cells.

Next we examined the expression patterns of molecules involved in lipid metabolism by using cDNA microarray and qPCR analyses. Although expression levels of low-density lipoprotein receptor (LDLR), sterol regulatory element-binding protein 1c (SREBP1c), SREBP2, and DGAT1 in nonhepatic Hec1B and 293T cells were comparable to those in hepatic Huh7 and Hep3B cells, those of VLDL-associated proteins, including ApoE, ApoB, and

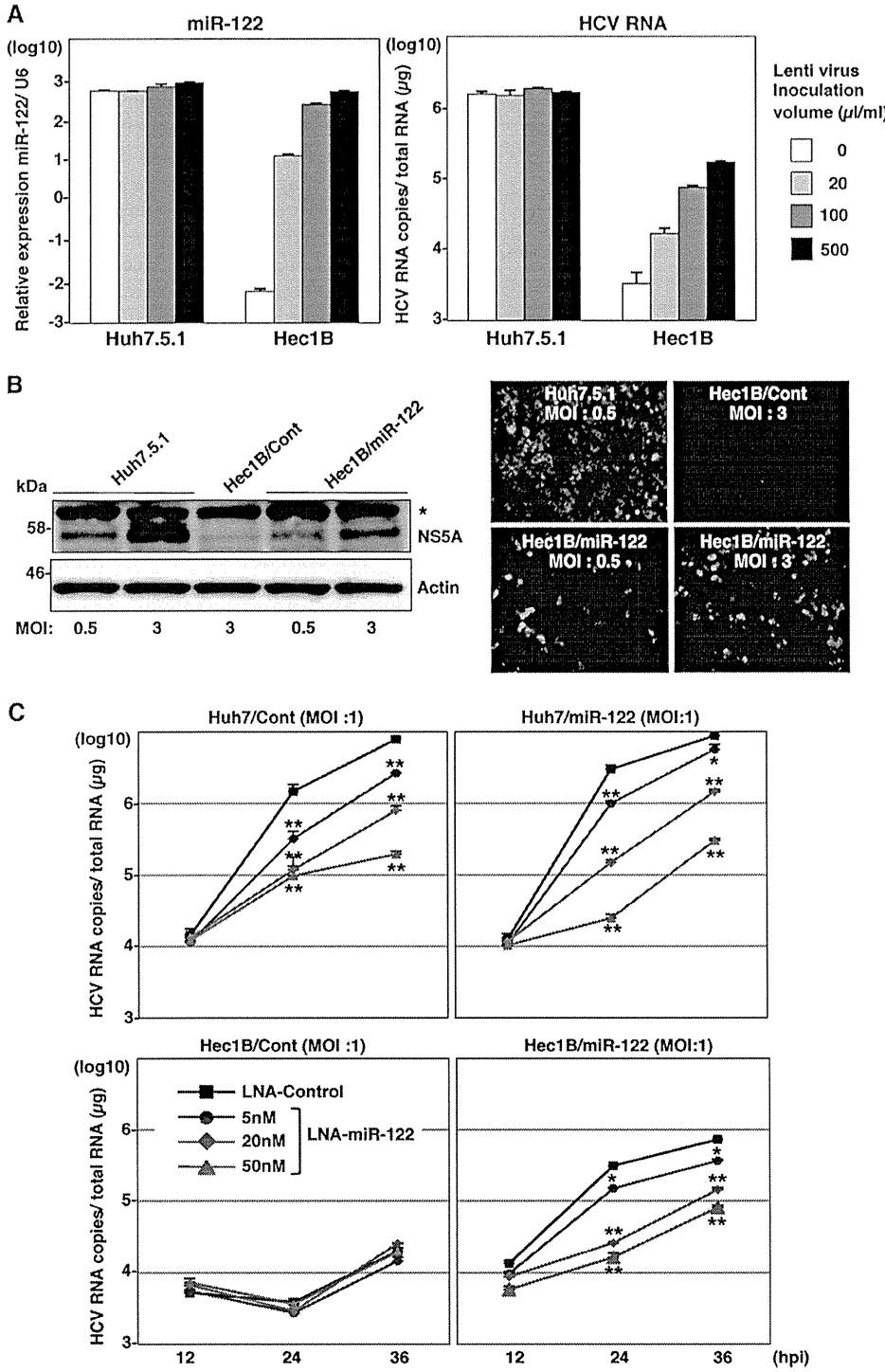


FIG 6 Expression of miR-122 is essential for the enhancement of HCV replication in the Hec1B cells. (A) Huh7.5.1 and Hec1B cells were transduced with lentiviral vectors expressing miR-122 in a dose-dependent manner and infected with HCVcc at an MOI of 1. Intracellular miR-122 and HCV RNA were determined at 24 h postinfection by qRT-PCR. (B) Huh7.5.1 and Hec1B/miR-122 cells were infected with HCVcc at an MOI of 0.5 or 3 and subjected to immunoblotting and immunofluorescence analyses using anti-NS5A antibodies at 48 h postinfection. The asterisk indicates nonspecific bands. (C) LNAs specific to miR-122 at a final concentration of 5 nM, 20 nM, or 50 nM and control (LNA alone at 50 nM) were introduced into Huh7/Cont, Huh7/miR-122, Hec1B/miR-122, and Hec1B/Cont cells by using Lipofectamine RNAiMAX transfection reagent and infected with HCVcc at an MOI of 1 at 6 h posttransfection. Intracellular HCV RNA levels were determined by qRT-PCR at 12, 24, and 36 h postinfection. Asterisks indicate significant differences (*, $P < 0.05$; **, $P < 0.01$) versus the results for control cells.